

Breaking Bad Molecules: Are MLLMs Ready for Structure-Level Molecular Detoxification?

Fei Lin^{1*} Ziyang Gong^{2,4*} Cong Wang^{3*} Yonglin Tian³
Tengchao Zhang¹ Xue Yang² Gen Luo⁴ Fei-Yue Wang^{1,3†}

¹Macau University of Science and Technology ²Shanghai Jiao Tong University
³Institute of Automation, Chinese Academy of Sciences ⁴Shanghai AI Laboratory

Abstract

Toxicity remains a leading cause of early-stage drug development failure. Despite advances in molecular design and property prediction, the task of *molecular toxicity repair*—generating structurally valid molecular alternatives with reduced toxicity—has not yet been systematically defined or benchmarked. To fill this gap, we introduce **ToxiMol**, the first benchmark task for general-purpose Multimodal Large Language Models (MLLMs) focused on molecular toxicity repair. We construct a standardized dataset covering 11 primary tasks and 560 representative toxic molecules spanning diverse mechanisms and granularities. We design a prompt annotation pipeline with mechanism-aware and task-adaptive capabilities, informed by expert toxicological knowledge. In parallel, we propose an automated evaluation framework, **ToxiEval**, which integrates toxicity endpoint prediction, synthetic accessibility, drug-likeness, and structural similarity into a high-throughput evaluation chain for repair success. We systematically assess nearly 30 mainstream general-purpose MLLMs and design multiple ablation studies to analyze key factors such as evaluation criteria, candidate diversity, and failure attribution. Experimental results show that although current MLLMs still face significant challenges on this task, they begin to demonstrate promising capabilities in toxicity understanding, semantic constraint adherence, and structure-aware molecule editing. The evaluation code and benchmark datasets are available at [this repository](#).

1 Introduction

In drug discovery, approximately 90% of candidate compounds fail due to poor Absorption, Distribution, Metabolism, Excretion, and Toxicity (ADMET) properties, with toxicity issues—such as hepatotoxicity, cardiotoxicity, and carcinogenicity—being among the primary causes of attrition during preclinical development [5–7]. Traditional toxicity mitigation strategies rely on structural modifications, scaffold replacement, or fragment-based optimization for small-molecule drugs [8–10]. These processes are not only heavily dependent on expert knowledge but also require extensive iterative experimentation, resulting in high complexity, long development cycles, and significant costs [11]. In recent years, the rapid advancement of multimodal fusion and Large Language Models (LLMs) has led to the emergence of general-purpose Multimodal

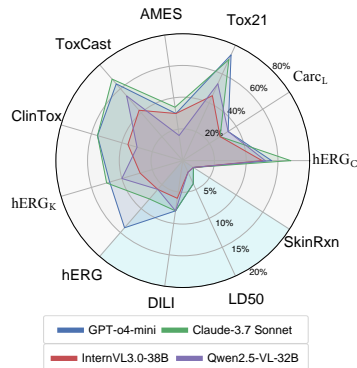


Figure 1: A radar plot of success rates (%) of representative MLLMs [1–4] across 11 toxicity repair tasks. To enhance visual contrast, the four low-performing tasks are highlighted in a light blue area with axes scaled to 0–20%, while other tasks use a 0–80% range.

*Equal Contribution.

†Corresponding author. Email: feiyue.wang@ia.ac.cn

Large Language Models (MLLMs [12–15]) with strong capabilities in cross-modal perception and reasoning [16]. These MLLMs are increasingly explored in highly structured scientific domains such as chemistry and life sciences [17, 18]. Against this backdrop, a critical question arises: do general-purpose MLLMs possess the capacity to recognize and repair toxic molecules, and can they effectively support the “detoxification” objectives of molecular design?

Recent studies have begun to explore the application of general-purpose MLLMs to tasks such as molecule grounding, toxicity prediction, and structure editing, achieving promising progress in various scenarios [19–24]. However, the task of molecular toxicity repair—a critical capability in drug design—has yet to be systematically defined, leaving a significant gap in current research. To address this, we introduce **ToxiMol**, the first comprehensive benchmark for molecular toxicity repair tailored to general-purpose MLLMs. This task extends beyond conventional domains such as toxicity prediction, ADMET modeling, and property-driven optimization [25–27], aiming to rigorously assess the ability of MLLMs to perform complex molecular structure refinement. Specifically, the task requires the model to take as input a toxic molecule represented by its Simplified Molecular Input Line Entry System (SMILES), 2D structural image, and a natural language description of the repair objective, then identify potential toxicity endpoints, interpret semantic constraints, and generate structurally similar substitute molecules that successfully eliminate toxic fragments while satisfying drug-likeness and synthetic feasibility requirements. This process poses multifaceted challenges to the model, including toxicological knowledge representation, fine-grained perception of molecular structure, semantic comprehension of complex instructions, and high-reliability response generation.

We construct a standardized molecular toxicity repair dataset by reselecting and integrating high-quality annotated samples from multiple toxicity prediction tasks on the Therapeutics Data Commons (TDC) platform [28–30] to evaluate this highly challenging and practically valuable task systematically. The dataset covers 11 primary tasks, with two of them containing 12 and 10 sub-tasks, respectively, and includes a total of 560 representative toxic molecules spanning diverse mechanisms and varying toxicity granularities. For each task, we design expert-informed prompt templates grounded in toxicological knowledge and build a mechanism-aware and task-adaptive prompt annotation pipeline. To enable automated, multi-dimensional, and objective evaluation of the generated molecules, we further propose an evaluation framework—**ToxiEval**—which integrates toxicity endpoint prediction, synthetic accessibility, drug-likeness scores, and structural similarity into a high-throughput molecular assessment chain for determining the success of toxicity repair.

We conducted a systematic evaluation of nearly 30 mainstream general-purpose MLLMs, including both closed-source and open-source models, and designed multiple ablation studies to analyze various aspects of the task. These include analysis of structural validity, strategies for combining multi-dimensional criteria, the influence of candidate set size, and failure mode attribution. Experimental results show that while the overall success rate of current general-purpose MLLMs on the toxicity repair task remains relatively low, the models have begun to demonstrate initial potential in addressing this challenging problem.

In summary, the main contributions of this work are as follows:

- **A novel task and challenge for general-purpose MLLMs.** We introduce **ToxiMol**, the first benchmark for *molecular toxicity repair*, as a new standard to evaluate the generalization and execution capabilities of general-purpose MLLMs on highly complex scientific problems.
- **A standardized toxicity repair dataset and automated evaluation framework.** We construct a benchmark dataset featuring diverse mechanisms and controllable granularity and propose **ToxiEval**, an automated, multi-dimensional evaluation framework that enables fair, transparent, and quantitative comparison of model performance under complex repair objectives.
- **Extensive evaluation and systematic analysis.** We conduct a comprehensive assessment of nearly 30 mainstream general-purpose MLLMs across multiple tasks, models, and evaluation criteria and perform in-depth ablation studies to examine the effects of various factors on repair success, revealing both the potential and current limitations of MLLMs in toxicity repair.

2 Related Work

Molecular Toxicity Repair. The molecular toxicity repair task lies at the intersection of two major research directions: molecular toxicity prediction and molecular structure editing. Traditional

toxicity prediction approaches rely on rule-based expert systems, Quantitative Structure-Activity Relationship (QSAR) models [31–33], and Graph Neural Networks (GNNs) [34, 35]. More recently, the rise of LLMs has introduced a new paradigm, with zero-shot models such as Tx-LLM [36], MoLE [37], and TxGemma [38] demonstrating strong cross-task generalization capabilities and significantly expanding the expressive framework of toxicity prediction. In contrast, molecular structure editing focuses on property-guided molecule reconstruction. Representative approaches include GNN-based property-driven editing [39, 40], molecular diffusion models [41, 42], and LLM-based structure generation [43, 44, 21, 45, 46]. These methods typically optimize for a single target property—such as solubility, permeability, or drug-likeness—by generating new structures that meet specific constraints.

In contrast, molecular toxicity repair remains in its early exploratory phase, treated as a standalone and **yet-to-be-systematically-defined** task paradigm. Traditional methods primarily rely on rule-based toxicophore databases such as ToxAlerts [47], which lack the capability for structure generation or automated repair [48, 49]. Recent studies have attempted to incorporate toxicity metrics into joint ADMET optimization frameworks [50]. Some works employ deep neural network models, such as Transformers, for ADMET property prediction and regression modeling [34, 51, 27, 52, 53], while others have begun to explore LLM-based multitask benchmarks for ADMET tasks [25, 46, 54]. However, there remains a lack of systematic approaches for modeling and evaluating the specific goal of “toxicity repair,” i.e., generating structurally valid, low-toxicity alternatives from toxic molecules.

MLLMs and QA Benchmarks. MLLMs have demonstrated remarkable capabilities in cross-modal semantic understanding tasks, with prominent proprietary models such as GPT [12, 55], Claude [56, 2], and Gemini [57–60], as well as open-source counterparts like BLIP [61, 62], LLaVA [63–65], Qwen-VL [15, 66], and InternVL [67, 68, 14, 69]. While these models perform strongly on general vision-language tasks, their generalization ability in molecular structure understanding and pharmaceutical applications remains significantly limited. To bridge this gap, researchers have proposed vertical-domain MLLMs tailored for chemistry and drug discovery tasks, aiming to improve their alignment with specialized objectives [70–74]. However, such adaptations often come at the cost of diminished general-purpose semantic modeling and reduced cross-task generalizability.

For the evaluation of general-purpose MLLMs, researchers have developed systematic benchmarks across various task dimensions, including image captioning, Visual Question Answering (VQA), and code generation [75, 16, 76]. In the chemistry and pharmaceutical domains, emerging benchmarks such as Molecule Captioning [77, 78], MolTextQA [79], Mol-Hallu [80], and MolPuzzle [81] have been proposed to assess model capabilities in molecular structure understanding, textual description, and task reasoning [82, 83]. However, no established benchmark remains for evaluating MLLMs in the critical setting of toxicity repair. To our knowledge, this work is the **first to introduce toxicity repair as a benchmark task for general-purpose MLLMs** and to systematically evaluate their performance in molecular structure optimization and image-based chemical analysis.

3 ToxiMol Benchmark

3.1 Overview

Task Definition. The ToxiMol Benchmark defines a toxicity repair task as follows: Given a toxicity-positive small molecule represented by its SMILES string $\text{SMILES}_i^{\text{raw}}$, its corresponding 2D molecular structure image IMG_i (rendered via RDKit [84] following international chemical depiction conventions, e.g., oxygen atoms in red, nitrogen in blue), and a repair prompt \mathcal{P}_i , these inputs are fed into a MLLM denoted as \mathcal{M} . The model is instructed to generate a set of three candidate repaired molecules, denoted by $\mathcal{S}_i^{\text{rep}} := \{\text{SMILES}_i^{\text{rep}(1)}, \text{SMILES}_i^{\text{rep}(2)}, \text{SMILES}_i^{\text{rep}(3)}\}$. If any of the candidate molecules in $\mathcal{S}_i^{\text{rep}}$ satisfies the multi-criteria evaluation defined by the ToxiEval framework, the repair is considered successful; otherwise, it is deemed a failure. The formal definition of this task is presented below.

$$(\text{SMILES}_i^{\text{raw}}, \text{IMG}_i, \mathcal{P}_i) \xrightarrow{\mathcal{M}} \mathcal{S}_i^{\text{rep}} \Rightarrow \text{Success}(i) = \begin{cases} 1, & \exists s \in \mathcal{S}_i^{\text{rep}} \text{ s.t. } \text{ToxiEval}(s) = 1 \\ 0, & \text{otherwise} \end{cases}$$

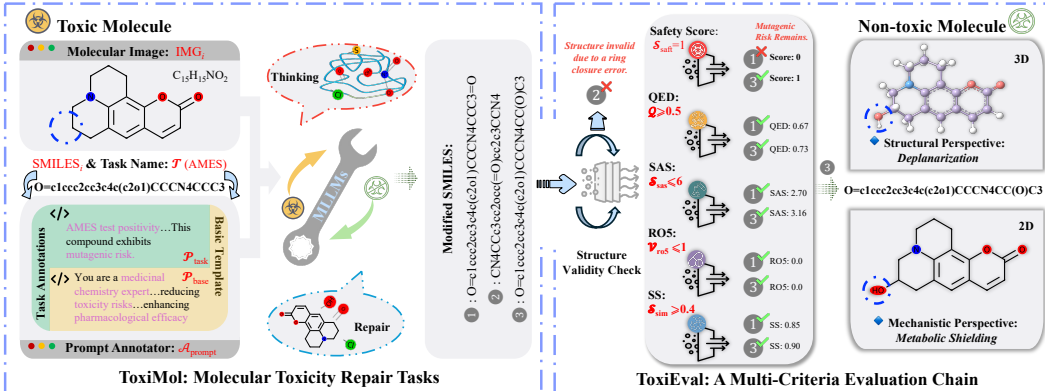


Figure 3: A repair example on the AMES task (binary classification, $\mathcal{S}_{\text{safe}} = 1$) using the ToxiMol benchmark. The input includes the SMILES of Coumarin 6H [102], its 2D molecular image, and a task-adaptive prompt annotation pipeline. After toxicity repair by the MLLM, three candidate molecules are generated. Due to structural invalidity, the ToxiEval evaluation chain first filters out Candidate 2. Among the remaining molecules, Candidate 1 is excluded for failing the safety threshold in the multi-criteria assessment. Candidate 3 passes all stages of the ToxiEval chain and is identified as a successful repair. Both 2D and 3D visualizations of the final output are presented.

chain tailored for toxicity repair scenarios. ToxiEval encompasses key evaluation dimensions, including structural validity, safety scoring, and drug-likeness, among others, aiming to systematically and fine-grainedly assess the real-world performance of general-purpose MLLMs on complex repair tasks. The overall execution flow of ToxiEval is illustrated in Fig. 3, with the corresponding algorithm detailed in Appendix G and H. Additional case examples are provided in Appendix O.

Structure Validity Check. Since the SMILES strings generated by general-purpose MLLMs do not always conform to syntactic standards, ToxiEval begins by invoking RDKit [84] to parse each candidate molecule. The molecule is deemed invalid and excluded from subsequent evaluation if the SMILES cannot be converted into a valid molecular graph. This step is positioned at the beginning of the evaluation pipeline to ensure the credibility of the results and to save computational resources.

Multi-Dimensional Evaluation Criteria and Decision Protocol. ToxiEval defines five core evaluation dimensions: Safety Score $\mathcal{S}_{\text{safe}}$, Quantitative Estimate of Drug-likeness (QED) \mathcal{Q} , Lipinski’s Rule of Five (RO5) \mathcal{V}_{ro5} , Synthetic Accessibility Score (SAS) \mathcal{S}_{sas} , and Structural Similarity (SS) \mathcal{S}_{sim} . See Appendix F for details on these evaluation metrics. We adopt a strict conjunctive decision protocol, where a generated molecule is deemed *successfully repaired* only if all criteria are satisfied simultaneously. The definitions and thresholds are as follows:

- **Safety Score:** We use the TxGemma-Predict [38] model to estimate toxicity endpoints. For binary classification tasks, label “A” (non-toxic/non-inhibitory) corresponds to $\mathcal{S}_{\text{safe}} = 1$, while label “B” (toxic/inhibitory) corresponds to $\mathcal{S}_{\text{safe}} = 0$, and the threshold is $\mathcal{S}_{\text{safe}} = 1$. For the LD50 task, the model outputs a continuous score in $[0, 1000]$, representing a lethal dose where higher values indicate lower toxicity. This score is normalized to $[0, 1]$, and the threshold is set to $\mathcal{S}_{\text{safe}} > 0.5$, consistent with the default decision boundary of TxGemma-Predict.
- **QED:** This criterion evaluates drug-likeness. QED outputs a continuous score in $[0, 1]$, with higher values, indicating a stronger resemblance to real drug compounds. Following Bickerton *et al.* [103], the threshold is $\mathcal{Q} \geq 0.5$.
- **SAS:** SAS assesses the synthetic feasibility of molecules, with scores ranging from $[1, 10]$. Lower values indicate easier synthesis. Based on Ertl and Schuffenhauer’s findings, we set the threshold as $\mathcal{S}_{\text{sas}} \leq 6$ [104].
- **RO5:** RO5 measures compliance with classic oral drug design rules based on properties such as molecular weight, LogP, and hydrogen bond donor/acceptor counts. As proposed by Lipinski *et al.* [105], the threshold is $\mathcal{V}_{\text{ro5}} \leq 1$.

Table 2: **Toxicity Repair Success Rates (%)**. hERGC, hERGK, and Carc_L refer to the hERG_Central, hERG_Karim, and Carcinogens tasks, respectively. SkinRxn denotes the SkinReaction task. Claude-3.7 Sonnet (20250219), Claude-3 Opus (20240229), and Gemini-2.5 pro-exp (20250325) indicate the specific model versions used for evaluation.

Models	LD50	hERGC	Carc _L	Tox21	AMES	ToxCast	ClinTox	DILI	hERG _K	hERG	SkinRxn	Overall
Close Source MLLMs												
GPT-o4-mini [1]	4.0	56.0	34.0	73.3	30.0	64.0	56.0	8.0	48.0	14.0	2.0	36.1
GPT-o3 [1]	6.0	48.0	34.0	75.0	32.0	66.0	56.0	6.0	50.0	10.0	0.0	35.5
GPT-o1 [107]	2.0	58.0	32.0	61.7	26.0	56.0	48.0	4.0	30.0	8.0	0.0	30.2
GPT-4.1 [108]	6.0	60.0	28.0	63.3	36.0	72.0	44.0	8.0	26.0	4.0	2.0	32.3
GPT-4o [55]	4.0	58.0	26.0	65.0	28.0	56.0	44.0	6.0	34.0	4.0	2.0	30.4
Claude-3.7 Sonnet Thinking [2]	4.0	60.0	34.0	63.3	36.0	68.0	66.0	4.0	38.0	16.0	0.0	35.9
Claude-3.7 Sonnet [2]	4.0	68.0	28.0	70.0	34.0	68.0	56.0	8.0	50.0	8.0	2.0	36.6
Claude-3 Opus [56]	2.0	64.0	34.0	66.7	30.0	62.0	52.0	10.0	30.0	6.0	2.0	33.2
Gemini-2.5 pro-exp [60]	4.0	70.0	30.0	68.3	30.0	62.0	56.0	4.0	42.0	14.0	4.0	35.5
Gemini-2.0 flash-thinking-exp [59]	0.0	54.0	20.0	60.0	22.0	54.0	32.0	2.0	28.0	12.0	0.0	26.4
Gemini-1.5-pro [58]	2.0	52.0	28.0	61.7	26.0	60.0	54.0	4.0	38.0	10.0	6.0	31.6
Grok-2-vision [109]	2.0	58.0	28.0	56.7	24.0	56.0	48.0	6.0	28.0	2.0	0.0	28.6
GLM-4v-plus [110]	0.0	32.0	14.0	48.3	14.0	42.0	22.0	0.0	12.0	2.0	2.0	17.7
Moonshot-v1-128k-vision [111]	6.0	50.0	26.0	50.0	22.0	50.0	40.0	8.0	32.0	8.0	2.0	27.1
hunyuan-vision [112]	2.0	24.0	20.0	36.7	12.0	46.0	26.0	2.0	14.0	0.0	0.0	17.0
Open Source MLLMs												
InternVL3.0-8B [14]	2.0	22.0	8.0	18.3	14.0	30.0	16.0	4.0	10.0	2.0	0.0	11.7
InternVL3.0-14B [3]	0.0	36.0	30.0	45.0	24.0	54.0	36.0	6.0	32.0	8.0	0.0	25.0
InternVL3.0-38B [3]	2.0	50.0	28.0	45.0	30.0	42.0	36.0	6.0	28.0	6.0	2.0	25.4
InternVL3.0-78B [69]	4.0	38.0	22.0	50.0	22.0	54.0	34.0	0.0	24.0	0.0	0.0	23.0
Qwen2.5-VL-7B-Instruct [4]	0.0	16.0	4.0	15.0	6.0	4.0	4.0	0.0	6.0	2.0	0.0	5.4
Qwen2.5-VL-32B-Instruct [4]	2.0	52.0	34.0	53.3	16.0	54.0	30.0	8.0	40.0	6.0	2.0	27.5
Qwen2.5-VL-72B-Instruct [4]	6.0	52.0	32.0	58.3	28.0	42.0	44.0	4.0	22.0	6.0	0.0	27.3
DeepSeek-VL2-tiny [113]	2.0	26.0	12.0	45.0	10.0	36.0	24.0	0.0	16.0	0.0	0.0	16.1
DeepSeek-VL2-small [113]	0.0	34.0	12.0	50.0	12.0	46.0	20.0	0.0	14.0	4.0	0.0	18.0
DeepSeek-VL2 [113]	2.0	30.0	14.0	45.0	16.0	38.0	28.0	2.0	10.0	0.0	0.0	17.3
LLaVA-OneVision-7B [114]	0.0	32.0	8.0	51.7	12.0	40.0	22.0	0.0	12.0	0.0	0.0	16.8
LLaVA-OneVision-72B [114]	0.0	42.0	28.0	53.3	24.0	40.0	26.0	0.0	16.0	2.0	0.0	21.6
Average Success Rate	2.5	46.0	24.0	53.7	22.8	50.4	37.8	4.1	27.0	5.7	1.0	25.5

- **SS**: Tanimoto similarity measures scaffold preservation between original and repaired molecules. Based on Rogers and Hahn, we set the threshold as $S_{\text{sim}} \geq 0.4$ [106].

4 Experiments

4.1 Benchmarking Procedure

We systematically evaluate the performance of mainstream closed- and open-source MLLMs across 11 primary toxicity repair tasks. Additionally, the 12 sub-tasks from Tox21 and 10 from ToxCast are included in extended evaluations (see Appendix I and J). All experiments are conducted under a unified testing environment equipped with 8 NVIDIA A800 GPUs. Each model operates under a single-round QA setting, generating exactly 3 repair candidates per sample. The temperature parameter is uniformly set to 0.7 for all MLLMs; default settings are used when this is not configurable. A unified evaluation criterion is applied: **a sample is successfully repaired if at least one candidate molecule passes the ToxiEval multi-dimensional evaluation chain**. Given that ToxiEval employs binary decision thresholds, we do not perform multiple sampling or report standard deviations. S_{safe} are computed using the TxGemma-9B-Predict [38] model loaded in float16 precision (for model size ablation, see Appendix L). The implementation details of Q , V_{ro5} , S_{sas} , and S_{sim} are provided in Appendix P. We report the per-task success rate and the overall success rate as the primary performance metrics.

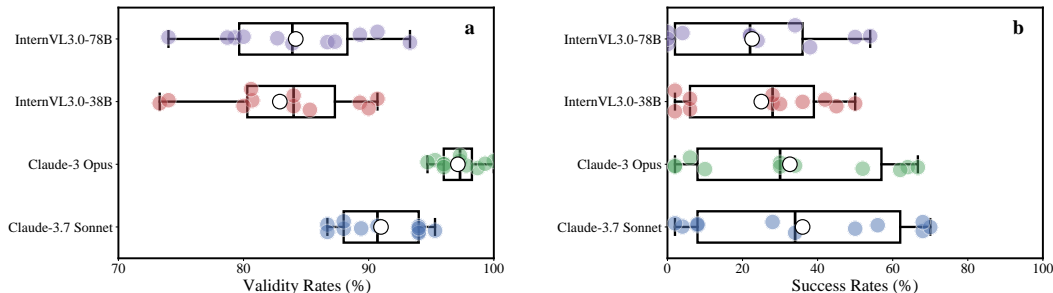


Figure 4: **Distribution of validity and success rates (%) of representative MLLMs on the ToxiMol benchmark.** Panel (a) shows the structural validity rates of each model, and panel (b) shows their repair success rates. Each dot represents a subtask, and the box plots reflect the distribution patterns and stability differences across tasks.

4.2 Overall Performance

Model-Level Insights. As shown in Table 2, the overall success rates of current general-purpose MLLMs remain relatively low, indicating that the task presents a significant challenge and leaves ample room for performance improvement. Notably, reasoning-enhanced models (e.g., GPT-o1/o3/o4-min [1, 107]) exhibit performance comparable to standard MLLMs (e.g., GPT-4.1/4o [108, 55]), suggesting that advanced reasoning capabilities have yet to translate into a clear advantage in this task. Among open-source models, performance appears to be more sensitive to model scale: lightweight models (e.g., 7B/8B) tend to underperform across most tasks. In contrast, larger models show progressively more stable results.

Task-Level Insights. General-purpose MLLMs achieve relatively higher success rates on Tox21 and ToxCast, suggesting a degree of generalization capability in handling toxicity phenotype classification tasks. In contrast, their performance is consistently lower on LD50, DILI, and SkinRxn. As a representative structural regression challenge, the LD50 task requires the model to capture continuous representations of dose-dependent toxicity during generation, posing higher demands on structural comprehension and mechanistic reasoning. The DILI task, involving hepatic metabolism and systemic toxicity, is driven by complex and multifactorial mechanisms that are difficult for current MLLMs to represent accurately. SkinRxn exhibits the lowest success rate, further exposing a critical bottleneck in MLLMs’ ability to reconstruct chemically induced skin toxicity pathways. Additionally, models perform significantly worse on the standard hERG task compared to hERG_C and hERG_K, despite their mechanistic proximity. As detailed in Appendix K, we conduct targeted ablation studies to investigate this discrepancy.

4.3 Ablation Studies

Structure Validity Analysis. We evaluate the structural validity of the repaired molecules generated by different MLLMs. The experiment includes 560 test samples, with 3 candidate molecules generated per sample, resulting in 1680 generated molecules. We present the results for Claude-3.7 Sonnet [2], Claude-3 Opus [56], and InternVL3.0-38B/78B [3, 69] in Fig. 4; results for other models are provided in Appendix M.

The results indicate that structure validity alone does not directly determine repair success. For example, Claude-3 Opus achieves a slightly higher validity rate than Claude-3.7 Sonnet, yet its repair success rate is lower, potentially due to a more conservative generation strategy that lacks effective avoidance of toxic mechanisms. Additionally, the InternVL 3.0 series exhibits comparable performance in both validity and success rates, suggesting diminishing marginal returns from further scaling up model size. In high-difficulty tasks such as SkinRxn, success rates remain extremely low even when validity is high, highlighting that structure validity is a necessary but insufficient condition for successful toxicity repair. Therefore, structure validity should serve as a preliminary filter within the ToxiEval evaluation pipeline, but not as the principal criterion for generation quality.

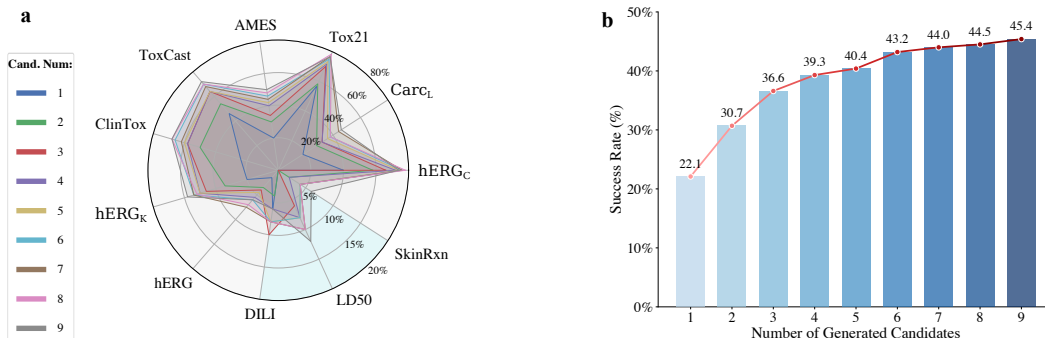


Figure 5: **Effect of candidate counts $k \in [1, 9]$ on toxicity repair success rates.** Panel (a) shows task-level success rates in a radar chart, with each color representing a candidate count. Three low-performing tasks are highlighted in a light blue area with axes scaled to 0–20%, while others use a 0–80% range. Panel (b) shows overall success rates as a function of candidate number.

Multi-Dimensional Metric Combination Analysis. The ToxiEval framework defines five core evaluation dimensions: $\mathcal{S}_{\text{safe}}$, \mathcal{Q} , \mathcal{V}_{ro5} , \mathcal{S}_{sas} , and \mathcal{S}_{sim} . To better understand the influence of these metric combinations on final success determination, we take Claude-3.7 Sonnet [2] as a case study and fix $\mathcal{S}_{\text{safe}}$ as a necessary condition. We then exhaustively evaluate all $2^4 = 16$ combinations of the remaining four dimensions and compute the overall success rate under each condition. The results are reported in Table 3.

Analysis results indicate that using $\mathcal{S}_{\text{safe}}$ as the sole evaluation criterion yields the highest overall success rate. Introducing any additional constraint leads to varying degrees of performance drop, with combinations involving \mathcal{Q} (QED) showing the most significant decline. This suggests that models tend to achieve toxicity mitigation at the cost of reduced drug-likeness. These findings offer practical guidance for evaluation design: in scenarios requiring rapid screening of candidate molecules, a lightweight evaluation scheme comprising $\mathcal{S}_{\text{safe}}$, \mathcal{S}_{sas} , and \mathcal{V}_{ro5} may suffice; whereas for applications demanding full assurance of drug development potential, retaining the complete five-dimensional constraint set is recommended.

Table 3: **Impact of Evaluation Metric Combinations on Success Rate.**

$\mathcal{S}_{\text{safe}}$	\mathcal{Q}	\mathcal{S}_{sas}	\mathcal{V}_{ro5}	\mathcal{S}_{sim}	Overall (%)
✓	✗	✗	✗	✗	53.2
✓	✓	✗	✗	✗	41.1
✓	✗	✓	✗	✗	52.9
✓	✗	✗	✓	✗	50.7
✓	✗	✗	✗	✓	48.6
✓	✓	✓	✗	✗	40.9
✓	✓	✗	✓	✗	41.1
✓	✓	✗	✗	✓	36.8
✓	✗	✓	✓	✗	50.5
✓	✗	✓	✗	✓	48.2
✓	✗	✗	✓	✓	46.1
✓	✓	✓	✓	✗	40.9
✓	✓	✓	✗	✓	36.6
✓	✓	✗	✓	✓	36.8
✓	✗	✓	✓	✓	45.9
✓	✓	✓	✓	✓	36.6

Effect of Candidate Molecule Count on Success Rate. To systematically analyze the impact of the number of generated candidates k on the success rate of toxicity repair, we select the Claude-3.7 Sonnet [2] model and vary $k \in [1, 9]$ by dynamically specifying the number of molecules to be generated in the prompt. Each set of generated results is evaluated consistently using the ToxiEval framework. Figure 5 presents the task-level radar charts (a) and the corresponding overall success rates (b) under different values of k .

Experimental results show that increasing the number of candidates significantly improves the success rate of toxicity repair, but with a clear diminishing marginal return. Since MLLMs have a limited understanding of toxicity mechanisms, the quality of generated molecules does not increase linearly, leading to a plateau in the overall success rate. At the task level, different tasks exhibit varying sensitivity to k . For multi-label tasks such as Tox21 and ToxCast, the success rate grows almost linearly with k , suggesting that increased structural diversity among candidates improves the likelihood of matching the target mechanism. In contrast, for complex representation tasks like LD50 and SkinRxn, the success rate improvement remains limited even when $k \geq 6$. This indicates that such tasks impose higher demands on structural generation quality and mechanistic modeling and that merely increasing the number of candidates cannot compensate for MLLMs’ limitations in semantic reasoning and molecular graph understanding.

Table 4: **Failure-mode attribution for Claude-3.7 Sonnet on each toxicity-repair task.** Percentages are calculated over all candidate molecules for each task.

Task	Type-T (%)	Type-O (%)	Dominant Bottleneck
LD50	46.0	2.0	Toxic-dose regression is difficult
hERG _C	19.3	18.7	Type-O and Type-T contribute almost equally
Carc _L	11.3	24.0	Type-O is the main bottleneck
Tox21	14.4	19.4	Type-O and Type-T contribute almost equally
AMES	19.3	33.3	Type-O dominates
ToxCast	10.0	26.0	Type-O dominates
ClinTox	22.0	18.0	Toxicity still slightly dominates
DILI	57.3	0.7	Highly resistant toxicity; Type-O play marginal roles
hERG _K	24.7	16.0	Toxicity bottleneck remains primary
hERG	62.7	2.0	Strict "block" criterion hinders repair (see Appendix K)
SkinRxn	40.0	0.0	Structural alerts are hard for the MLLM to recognize

Failure Mode Attribution: Toxicity Bottleneck or Drug-Likeness Bottleneck? To further analyze the causes of failure for candidate molecules generated by MLLMs in the ToxiEval framework, we categorize unsuccessful samples into two distinct types:

- **Type-T (Toxicity Bottleneck):** All non-toxicity criteria are satisfied, but the safety score $\mathcal{S}_{\text{safe}} \neq 1$ (for binary tasks) or $\mathcal{S}_{\text{safe}} \leq 0.5$ (for the LD50 task), resulting in a failed repair decision.
- **Type-O (Drug-Likeness Bottleneck):** The toxicity is mitigated. Still, the candidate fails due to at least one of the \mathcal{Q} , \mathcal{S}_{sas} , \mathcal{V}_{ro5} , or \mathcal{S}_{sim} criteria not meeting the corresponding threshold.

We annotate whether each candidate molecule is successfully repaired. Table 4 reports the proportions (%) of two failure types for Claude-3.7 Sonnet [2] across 11 toxicity repair tasks. The results reveal several key insights:

Toxicity endpoints remain the primary bottleneck. The dominance of Type-T failures indicates that at least one candidate molecule, in most cases, satisfies the drug-likeness constraints, but successful toxicity repair is more complicated. In tasks like hERG, DILI, and SkinRxn, over 40% of failed candidates were rejected solely due to insufficient safety scores, highlighting the MLLMs’ lack of knowledge regarding specific toxicity mechanisms or potential weaknesses in the evaluation model. **Drug-likeness bottlenecks vary across tasks.** Type-O failures are more prevalent in Carc_L, AMES, and ToxCast tasks; while models can reduce toxicity, they often generate molecules with poor drug-likeness or feasibility. This observation aligns with the ablation findings in Table 3, where QED (\mathcal{Q}) exerted the most substantial filtering effect on repair success.

5 Findings and Open Directions

We conducted a systematic empirical evaluation and in-depth analysis, uncovering the performance bottlenecks and potential strengths of current MLLMs on the toxicity repair task. We believe that fostering deeper integration between AI and molecular science will facilitate the development of safer paradigms for molecule generation. Although the ToxiEval framework already covers various representative toxicity repair tasks, there remains substantial room for expansion along the task dimension. The current focus on structural repair reflects only part of the broader landscape of toxicity mitigation strategies, which in real-world applications may also involve dose regulation, release mechanism optimization, and metabolic pathway avoidance. Moreover, while this study concentrates on small-molecule drugs, toxicity assessment and repair for macromolecular systems—such as peptides, proteins, Antibody-Drug Conjugates (ADCs), and vaccines—are considerably more complex and warrant future exploration and extension. For additional discussions, see Appendix N.

6 Conclusion

This work systematically investigates the capability boundaries of general-purpose MLLMs on the *molecular toxicity repair task* and proposes a new multimodal, multi-objective benchmark—**ToxiMol**. The benchmark covers many real-world toxicity mechanisms, provides a standardized dataset, and introduces a complementary multi-criteria evaluation framework, **ToxiEval**. Experimental results show that although existing MLLMs have not explicitly been optimized for this task, they already demonstrate preliminary potential in toxicity mitigation. We hope this work provides a new task platform, evaluation benchmark, and research direction for general-purpose MLLMs, facilitating their advancement in the broader field of scientific intelligence.

References

- [1] OpenAI. Introducing o3 and o4-mini. <https://openai.com/blog/introducing-o3-and-o4-mini>, 2024. Accessed: 2025-05-05.
- [2] Anthropic. Claude 3.7 sonnet: New levels of intelligence and usefulness. <https://www.anthropic.com/news/claude-3-7-sonnet>, 2024. Accessed: 2025-05-05.
- [3] Jinguo Zhu and Weiyun et al. Wang. Internvl3: Exploring advanced training and test-time recipes for open-source multimodal models. *arXiv preprint arXiv:2504.10479*, 2025.
- [4] Shuai Bai, Keqin Chen, Xuejing Liu, Jialin Wang, Wenbin Ge, Sibao Song, Kai Dang, Peng Wang, Shijie Wang, Jun Tang, et al. Qwen2. 5-vl technical report. *arXiv preprint arXiv:2502.13923*, 2025.
- [5] Duxin Sun, Wei Gao, Hongxiang Hu, and Simon Zhou. Why 90% of clinical drug development fails and how to improve it? *Acta Pharmaceutica Sinica B*, 12(7):3049–3062, 2022.
- [6] Albert P Li. Accurate prediction of human drug toxicity: a major challenge in drug development. *Chemico-biological interactions*, 150(1):3–7, 2004.
- [7] Gail A Van Norman. Limitations of animal studies for predicting toxicity in clinical trials: is it time to rethink our current approach? *JACC: Basic to Translational Science*, 4(7):845–854, 2019.
- [8] Alaa-Eldin F Nassar, Amin M Kamel, and Caroline Clarimont. Improving the decision-making process in structural modification of drug candidates: reducing toxicity. *Drug Discovery Today*, 9(24):1055–1064, 2004.
- [9] Elwood A Mullins, Rongxin Shi, and Brandt F Eichman. Toxicity and repair of dna adducts produced by the natural product yatakemycin. *Nature chemical biology*, 13(9):1002–1008, 2017.
- [10] Fabian Dey and Amedeo Caffisch. Fragment-based de novo ligand design by multiobjective evolutionary optimization. *Journal of chemical information and modeling*, 48(3):679–690, 2008.
- [11] Anna O Basile, Alexandre Yahi, and Nicholas P Tatonetti. Artificial intelligence for drug toxicity and safety. *Trends in pharmacological sciences*, 40(9):624–635, 2019.
- [12] OpenAI. GPT-4V System Card, 2024. URL <https://openai.com/index/gpt-4v-system-card/>. Accessed: 2024-11-16.
- [13] Gen Luo, Xue Yang, Wenhan Dou, Zhaokai Wang, Jiawen Liu, Jifeng Dai, Yu Qiao, and Xizhou Zhu. Mono-internvl: Pushing the boundaries of monolithic multimodal large language models with endogenous visual pre-training. *arXiv preprint arXiv:2410.08202*, 2024.
- [14] OpenGVLab. Internvl 3.0-8b: An open multimodal large language model. <https://github.com/OpenGVLab/InternVL>, 2024. Accessed: 2025-05-05.
- [15] Jinze Bai and Shuai Bai et al. Qwen-vl: A versatile vision-language model for understanding, localization, text reading, and beyond, 2023.

- [16] Jiayi Kuang, Ying Shen, Jingyou Xie, Haohao Luo, Zhe Xu, Ronghao Li, Yinghui Li, Xianfeng Cheng, Xika Lin, and Yu Han. Natural language understanding and inference with mllm in visual question answering: A survey. *ACM Computing Surveys*, 57(8):1–36, 2025.
- [17] Mayk Caldas Ramos, Christopher J Collison, and Andrew D White. A review of large language models and autonomous agents in chemistry. *Chemical Science*, 2025.
- [18] Shi Xuan Leong, Sergio Pablo-García, Zijian Zhang, and Alán Aspuru-Guzik. Automated electrosynthesis reaction mining with multimodal large language models (mllms). *Chemical Science*, 15(43):17881–17891, 2024.
- [19] Jiaxin Wu, Ting Zhang, Rubing Chen, Wengyu Zhang, Chen Jason Zhang, Xiaoyong Wei, and Li Qing. Molground: A benchmark for molecular grounding. *arXiv preprint arXiv:2503.23668*, 2025.
- [20] Hengzheng Yang, Jian Xiu, Weiqi Yan, Kaifeng Liu, Huizi Cui, Zhibang Wang, Qizheng He, Yilin Gao, and Weiwei Han. Large language models as tools for molecular toxicity prediction: Ai insights into cardiotoxicity. *Journal of Chemical Information and Modeling*, 65(5):2268–2282, 2025.
- [21] Haorui Li, Shengchao Liu, Hongyu Guo, and Anima Anandkumar. Geometry-text multi-modal foundation model for reactivity-oriented molecule editing. In *NeurIPS 2024 Workshop on AI for New Drug Modalities*, 2024.
- [22] Yunhui Jang, Jaehyung Kim, and Sungsoo Ahn. Chain-of-thoughts for molecular understanding. *arXiv preprint arXiv:2410.05610*, 2024.
- [23] Zohar Rosenwasser, Erez Levanon, Michael Levitt, and Gal Oren. Leveraging gpt continual fine-tuning for improved rna editing site prediction. In *ICLR 2025 Workshop on Machine Learning for Genomics Explorations*, 2025.
- [24] Qitan Lv, Tianyu Liu, and Hong Wang. Exploiting edited large language models as general scientific optimizers. *arXiv preprint arXiv:2503.09620*, 2025.
- [25] Zhangming Niu, Xianglu Xiao, Wenfan Wu, Qiwei Cai, Yinghui Jiang, Wangzhen Jin, Minhao Wang, Guojian Yang, Lingkang Kong, Xurui Jin, et al. Pharmabench: Enhancing admet benchmarks with large language models. *Scientific Data*, 11(1):985, 2024.
- [26] Nicholas Aksamit, Alain Tchagang, Yifeng Li, and Beatrice Ombuki-Berman. Hybrid fragment-smiles tokenization for admet prediction in drug discovery. *BMC bioinformatics*, 25(1):255, 2024.
- [27] Alessio Fallani, Ramil Nugmanov, Jose Arjona-Medina, Jörg Kurt Wegner, Alexandre Tkatchenko, and Kostiantyn Chernichenko. Pretraining graph transformers with atom-in-a-molecule quantum properties for improved admet modeling. *Journal of Cheminformatics*, 17(1):25, 2025.
- [28] Alejandro Velez-Arce, Kexin Huang, Michelle M Li, Xiang Lin, Wenhao Gao, Tianfan Fu, Manolis Kellis, Bradley L Pentelute, and Marinka Zitnik. Tdc-2: Multimodal foundation for therapeutic science. *bioRxiv*, pages 2024–06, 2024.
- [29] Kexin Huang, Tianfan Fu, Wenhao Gao, Yue Zhao, Yusuf Roohani, Jure Leskovec, Connor W Coley, Cao Xiao, Jimeng Sun, and Marinka Zitnik. Therapeutics data commons: Machine learning datasets and tasks for drug discovery and development. *arXiv preprint arXiv:2102.09548*, 2021.
- [30] Kexin Huang, Tianfan Fu, Wenhao Gao, Yue Zhao, Yusuf Roohani, Jure Leskovec, Connor W Coley, Cao Xiao, Jimeng Sun, and Marinka Zitnik. Artificial intelligence foundation for therapeutic science. *Nature chemical biology*, 18(10):1033–1036, 2022.
- [31] Nigel Greene. Computer systems for the prediction of toxicity: an update. *Advanced Drug Delivery Reviews*, 54(3):417–431, 2002.

- [32] Mojca Fuart Gatnik and Andrew P Worth. *Review of software tools for toxicity prediction*. Publications Office of the European Union Luxembourg, 2010.
- [33] Romualdo Benigni and Cecilia Bossa. Predictivity of qsar. *Journal of chemical information and modeling*, 48(5):971–980, 2008.
- [34] Samar Monem, Alaa H Abdel-Hamid, and Aboul Ella Hassanien. Drug toxicity prediction model based on enhanced graph neural network. *Computers in Biology and Medicine*, 185: 109614, 2025.
- [35] Changsen Bai, Lianlian Wu, Ruijiang Li, Yang Cao, Song He, and Xiaochen Bo. Machine learning-enabled drug-induced toxicity prediction. *Advanced Science*, page 2413405, 2025.
- [36] Juan Manuel Zambrano Chaves, Eric Wang, Tao Tu, Eeshit Dhaval Vaishnav, Byron Lee, S Sara Mahdavi, Christopher Semturs, David Fleet, Vivek Natarajan, and Shekoofeh Azizi. Tx-llm: A large language model for therapeutics. *arXiv preprint arXiv:2406.06316*, 2024.
- [37] Oscar Méndez-Lucio, Christos A Nicolaou, and Berton Earnshaw. Mole: a foundation model for molecular graphs using disentangled attention. *Nature Communications*, 15(1):9431, 2024.
- [38] Eric Wang, Samuel Schmidgall, Paul F Jaeger, Fan Zhang, Rory Pilgrim, Yossi Matias, Joelle Barral, David Fleet, and Shekoofeh Azizi. Txgemma: Efficient and agentic llms for therapeutics. *arXiv preprint arXiv:2504.06196*, 2025.
- [39] Pietro Bongini, Monica Bianchini, and Franco Scarselli. Molecular generative graph neural networks for drug discovery. *Neurocomputing*, 450:242–252, 2021.
- [40] Odin Zhang, Haitao Lin, Hui Zhang, Huifeng Zhao, Yufei Huang, Chang-Yu Hsieh, Peichen Pan, and Tingjun Hou. Deep lead optimization: Leveraging generative ai for structural modification. *Journal of the American Chemical Society*, 146(46):31357–31370, 2024.
- [41] Jianmin Wang, Peng Zhou, Zixu Wang, Wei Long, Yangyang Chen, Kyoung Tai No, Dongsheng Ouyang, Jiashun Mao, and Xiangxiang Zeng. Diffusion-based generative drug-like molecular editing with chemical natural language. *Journal of Pharmaceutical Analysis*, page 101137, 2024.
- [42] Arne Schneuing, Charles Harris, Yuanqi Du, Kieran Didi, Arian Jamasb, Ilia Igashov, Weitao Du, Carla Gomes, Tom L Blundell, Pietro Lio, et al. Structure-based drug design with equivariant diffusion models. *Nature Computational Science*, 4(12):899–909, 2024.
- [43] Shengchao Liu, Weili Nie, Chengpeng Wang, Jiarui Lu, Zhuoran Qiao, Ling Liu, Jian Tang, Chaowei Xiao, and Animashree Anandkumar. Multi-modal molecule structure–text model for text-based retrieval and editing. *Nature Machine Intelligence*, 5(12):1447–1457, 2023.
- [44] Shengchao Liu, Jiong Xiao Wang, Yijin Yang, Chengpeng Wang, Ling Liu, Hongyu Guo, and Chaowei Xiao. Conversational drug editing using retrieval and domain feedback. In *The twelfth international conference on learning representations*, 2024.
- [45] Reza Averly, Frazier N Baker, and Xia Ning. Liddia: Language-based intelligent drug discovery agent. *arXiv preprint arXiv:2502.13959*, 2025.
- [46] Geyan Ye, Xibao Cai, Houtim Lai, Xing Wang, Junhong Huang, Longyue Wang, Wei Liu, and Xiangxiang Zeng. Drugassist: A large language model for molecule optimization. *Briefings in Bioinformatics*, 26(1):bbae693, 2025.
- [47] Iurii Sushko, Elena Salmina, Vladimir A Potemkin, Gennadiy Poda, and Igor V Tetko. Toxalerts: a web server of structural alerts for toxic chemicals and compounds with potential adverse reactions, 2012.
- [48] Emanuel SR Ehmki, Robert Schmidt, Farina Ohm, and Matthias Rarey. Comparing molecular patterns using the example of smarts: applications and filter collection analysis. *Journal of Chemical Information and Modeling*, 59(6):2572–2586, 2019.

- [49] Robert Schmidt, Emanuel SR Ehmki, Farina Ohm, Hans-Christian Ehrlich, Andriy Mashychev, and Matthias Rarey. Comparing molecular patterns using the example of smarts: theory and algorithms. *Journal of Chemical Information and Modeling*, 59(6):2560–2571, 2019.
- [50] Bing-Xue Du, Yi Xu, Siu-Ming Yiu, Hui Yu, and Jian-Yu Shi. Admet property prediction via multi-task graph learning under adaptive auxiliary task selection. *Iscience*, 26(11), 2023.
- [51] Lijuan Yang, Chao Jin, Guanghui Yang, Zhitong Bing, Liang Huang, Yuzhen Niu, and Lei Yang. Transformer-based deep learning method for optimizing admet properties of lead compounds. *Physical Chemistry Chemical Physics*, 25(3):2377–2385, 2023.
- [52] Krishna C Bulusu, Rajarshi Guha, Daniel J Mason, Richard PI Lewis, Eugene Muratov, Yasaman Kalantar Motamedi, Murat Cokol, and Andreas Bender. Modelling of compound combination effects and applications to efficacy and toxicity: state-of-the-art, challenges and perspectives. *Drug discovery today*, 21(2):225–238, 2016.
- [53] Marinka Zitnik, Monica Agrawal, and Jure Leskovec. Modeling polypharmacy side effects with graph convolutional networks. *Bioinformatics*, 34(13):i457–i466, 2018.
- [54] Raghad J AbuNasser, Mostafa Z Ali, Yaser Jararweh, Mustafa Daraghme, and Talal Z Ali. Large language models in drug discovery: A comprehensive analysis of drug-target interaction prediction. In *2024 2nd International Conference on Foundation and Large Language Models (FLLM)*, pages 417–431. IEEE, 2024.
- [55] Aaron Hurst and Adam et al. Lerer. Gpt-4o system card. *arXiv preprint arXiv:2410.21276*, 2024.
- [56] Anthropic. The claude 3 model family. <https://www.anthropic.com/news/claude-3-family>, 2024. Accessed: 2025-05-05.
- [57] Gemini Team, Rohan Anil, Sebastian Borgeaud, Jean-Baptiste Alayrac, Jiahui Yu, Radu Soricut, Johan Schalkwyk, Andrew M Dai, Anja Hauth, Katie Millican, et al. Gemini: a family of highly capable multimodal models. *arXiv preprint arXiv:2312.11805*, 2023.
- [58] Gemini Team and Petko et al. Georgiev. Gemini 1.5: Unlocking multimodal understanding across millions of tokens of context. *arXiv preprint arXiv:2403.05530*, 2024.
- [59] Google DeepMind. Gemini 2.0 flash thinking experimental. <https://ai.google.dev/gemini-api/docs/thinking>, 2025. Accessed: May 5, 2025.
- [60] Google DeepMind. Gemini 2.5 pro experimental: Google’s most advanced multimodal ai model. <https://blog.google/technology/google-deepmind/gemini-model-thinking-updates-march-2025/>, 2025. Accessed: May 5, 2025.
- [61] Junnan Li, Dongxu Li, Caiming Xiong, and Steven Hoi. Blip: Bootstrapping language-image pre-training for unified vision-language understanding and generation. In *International conference on machine learning*, pages 12888–12900. PMLR, 2022.
- [62] Junnan Li, Dongxu Li, Silvio Savarese, and Steven Hoi. Blip-2: Bootstrapping language-image pre-training with frozen image encoders and large language models. In *International conference on machine learning*, pages 19730–19742. PMLR, 2023.
- [63] Haotian Liu, Chunyuan Li, Qingyang Wu, and Yong Jae Lee. Visual instruction tuning. *Advances in neural information processing systems*, 36, 2024.
- [64] Haotian Liu, Chunyuan Li, Yuheng Li, and Yong Jae Lee. Improved baselines with visual instruction tuning. In *Proceedings of the IEEE/CVF Conference on Computer Vision and Pattern Recognition*, pages 26296–26306, 2024.
- [65] Haotian Liu, Chunyuan Li, Yuheng Li, Bo Li, Yuanhan Zhang, Sheng Shen, and Yong Jae Lee. Llava-next: Improved reasoning, ocr, and world knowledge, January 2024. URL <https://llava-vl.github.io/blog/2024-01-30-llava-next/>. Accessed: 2024-11-16.

- [66] Peng Wang, Shuai Bai, Sinan Tan, Shijie Wang, Zhihao Fan, Jinze Bai, Keqin Chen, Xuejing Liu, Jialin Wang, Wenbin Ge, et al. Qwen2-vl: Enhancing vision-language model’s perception of the world at any resolution. *arXiv preprint arXiv:2409.12191*, 2024.
- [67] Dongchen Lu, Yuyao Sun, Zilu Zhang, Leping Huang, Jianliang Zeng, Mao Shu, and Huo Cao. Internvl-x: Advancing and accelerating internvl series with efficient visual token compression. *arXiv preprint arXiv:2503.21307*, 2025.
- [68] Zhe Chen, Jiannan Wu, Wenhai Wang, Weijie Su, Guo Chen, Sen Xing, Muyan Zhong, Qinglong Zhang, Xizhou Zhu, Lewei Lu, et al. Internvl: Scaling up vision foundation models and aligning for generic visual-linguistic tasks. In *Proceedings of the IEEE/CVF conference on computer vision and pattern recognition*, pages 24185–24198, 2024.
- [69] OpenGVLab. Internvl 3.0-78b: Large-scale vision-language model by opengvlab. <https://github.com/OpenGVLab/InternVL>, 2024. Accessed: 2025-05-05.
- [70] Chanhui Lee, Yuheon Song, YongJun Jeong, Hanbum Ko, Rodrigo Hormazabal, Sehui Han, Kyunghoon Bae, Sungbin Lim, and Sungwoong Kim. Mol-llm: Generalist molecular llm with improved graph utilization. *arXiv preprint arXiv:2502.02810*, 2025.
- [71] Yizhen Luo, Jiahuan Zhang, Siqi Fan, Kai Yang, Yushuai Wu, Mu Qiao, and Zaiqing Nie. Biomedgpt: Open multimodal generative pre-trained transformer for biomedicine. *arXiv preprint arXiv:2308.09442*, 2023.
- [72] Yanjun Lyu, Zihao Wu, Lu Zhang, Jing Zhang, Yiwei Li, Wei Ruan, Zhengliang Liu, Xiaowei Yu, Chao Cao, Tong Chen, et al. Gp-gpt: Large language model for gene-phenotype mapping. *arXiv preprint arXiv:2409.09825*, 2024.
- [73] Yingheng Tang, Wenbin Xu, Jie Cao, Jianzhu Ma, Weilu Gao, Steve Farrell, Benjamin Erichson, Michael W Mahoney, Andy Nonaka, and Zhi Yao. Matterchat: A multi-modal llm for material science. *arXiv preprint arXiv:2502.13107*, 2025.
- [74] Dongki Kim, Wonbin Lee, and Sung Ju Hwang. Mol-llama: Towards general understanding of molecules in large molecular language model. *arXiv preprint arXiv:2502.13449*, 2025.
- [75] Jihyung Kil, Zheda Mai, Justin Lee, Arpita Chowdhury, Zihe Wang, Kerrie Cheng, Lemeng Wang, Ye Liu, and Wei-Lun Harry Chao. Mllm-compbench: A comparative reasoning benchmark for multimodal llms. *Advances in Neural Information Processing Systems*, 37: 28798–28827, 2024.
- [76] Chengyue Wu, Yixiao Ge, Qiushan Guo, Jiahao Wang, Zhixuan Liang, Zeyu Lu, Ying Shan, and Ping Luo. Plot2code: A comprehensive benchmark for evaluating multi-modal large language models in code generation from scientific plots. *arXiv preprint arXiv:2405.07990*, 2024.
- [77] Sihang Li, Zhiyuan Liu, Yanchen Luo, Xiang Wang, Xiangnan He, Kenji Kawaguchi, Tat-Seng Chua, and Qi Tian. Towards 3d molecule-text interpretation in language models. *arXiv preprint arXiv:2401.13923*, 2024.
- [78] Sumin Ha, Jun Hyeong Kim, Yinhua Piao, and Sun Kim. Mv-clam: Multi-view molecular interpretation with cross-modal projection via language model. *arXiv preprint arXiv:2503.04780*, 2025.
- [79] Siddhartha Laghuvarapu, Namkyeong Lee, Chufan Gao, and Jimeng Sun. MoltexQA: A curated question-answering dataset and benchmark for molecular structure-text relationship learning, 2024. URL <https://openreview.net/forum?id=gwGHBD9ZKU>.
- [80] Hao Li, Liuzhenghao Lv, He Cao, Zijing Liu, Zhiyuan Yan, Yu Wang, Yonghong Tian, Yu Li, and Li Yuan. How to detect and defeat molecular mirage: A metric-driven benchmark for hallucination in llm-based molecular comprehension. *arXiv preprint arXiv:2504.12314*, 2025.
- [81] Kehan Guo, Bozhao Nan, Yujun Zhou, Taicheng Guo, Zhichun Guo, Mihir Surve, Zhenwen Liang, Nitesh Chawla, Olaf Wiest, and Xiangliang Zhang. Can llms solve molecule puzzles? a multimodal benchmark for molecular structure elucidation. *Advances in Neural Information Processing Systems*, 37:134721–134746, 2024.

- [82] Yuqing Huang, Rongyang Zhang, Xuesong He, Xuyang Zhi, Hao Wang, Xin Li, Feiyang Xu, Deguang Liu, Huadong Liang, Yi Li, et al. Chemeval: A comprehensive multi-level chemical evaluation for large language models. *arXiv preprint arXiv:2409.13989*, 2024.
- [83] Junxian Li, Di Zhang, Xunzhi Wang, Zeying Hao, Jingdi Lei, Qian Tan, Cai Zhou, Wei Liu, Yaotian Yang, Xinrui Xiong, et al. Chemvlm: Exploring the power of multimodal large language models in chemistry. In *Proceedings of the AAAI Conference on Artificial Intelligence*, volume 39, pages 415–423, 2025.
- [84] Greg Landrum et al. Rdkit: Open-source cheminformatics. <https://www.rdkit.org>, 2024. Accessed: 2025-05-11.
- [85] Ruili Huang, Menghang Xia, Dac-Trung Nguyen, Tongan Zhao, Srilatha Sakamuru, Jinghua Zhao, Sampada A Shahane, Anna Rossoshek, and Anton Simeonov. Tox21challenge to build predictive models of nuclear receptor and stress response pathways as mediated by exposure to environmental chemicals and drugs. *Frontiers in Environmental Science*, 3:85, 2016.
- [86] Ann M Richard, Richard S Judson, Keith A Houck, Christopher M Grulke, Patra Volarath, Inthirany Thillainadarajah, Chihae Yang, James Rathman, Matthew T Martin, John F Wambaugh, et al. Toxcast chemical landscape: paving the road to 21st century toxicology. *Chemical research in toxicology*, 29(8):1225–1251, 2016.
- [87] Congying Xu, Feixiong Cheng, Lei Chen, Zheng Du, Weihua Li, Guixia Liu, Philip W Lee, and Yun Tang. In silico prediction of chemical ames mutagenicity. *Journal of chemical information and modeling*, 52(11):2840–2847, 2012.
- [88] Shuangquan Wang, Huiyong Sun, Hui Liu, Dan Li, Youyong Li, and Tingjun Hou. Admet evaluation in drug discovery. 16. predicting herg blockers by combining multiple pharmacophores and machine learning approaches. *Molecular pharmaceutics*, 13(8):2855–2866, 2016.
- [89] Abdul Karim, Matthew Lee, Thomas Balle, and Abdul Sattar. Cardiotox net: a robust predictor for herg channel blockade based on deep learning meta-feature ensembles. *Journal of cheminformatics*, 13:1–13, 2021.
- [90] Fang Du, Haibo Yu, Beiyang Zou, Joseph Babcock, Shunyou Long, and Min Li. hergcentral: a large database to store, retrieve, and analyze compound-human ether-a-go-go related gene channel interactions to facilitate cardiotoxicity assessment in drug development. *Assay and drug development technologies*, 9(6):580–588, 2011.
- [91] Alexey Lagunin, Dmitrii Filimonov, Alexey Zakharov, Wei Xie, Ying Huang, Fucheng Zhu, Tianxiang Shen, Jianhua Yao, and Vladimir Poroikov. Computer-aided prediction of rodent carcinogenicity by pass and cisoc-psct. *QSAR & Combinatorial Science*, 28(8):806–810, 2009.
- [92] Feixiong Cheng, Weihua Li, Yadi Zhou, Jie Shen, Zengrui Wu, Guixia Liu, Philip W Lee, and Yun Tang. admetsar: a comprehensive source and free tool for assessment of chemical admet properties, 2012.
- [93] Vinicius M Alves, Eugene Muratov, Denis Fourches, Judy Strickland, Nicole Kleinstreuer, Carolina H Andrade, and Alexander Tropsha. Predicting chemically-induced skin reactions. part i: Qsar models of skin sensitization and their application to identify potentially hazardous compounds. *Toxicology and applied pharmacology*, 284(2):262–272, 2015.
- [94] Youjun Xu, Ziwei Dai, Fangjin Chen, Shuaishi Gao, Jianfeng Pei, and Luhua Lai. Deep learning for drug-induced liver injury. *Journal of chemical information and modeling*, 55(10):2085–2093, 2015.
- [95] Hao Zhu, Todd M Martin, Lin Ye, Alexander Sedykh, Douglas M Young, and Alexander Tropsha. Quantitative structure- activity relationship modeling of rat acute toxicity by oral exposure. *Chemical research in toxicology*, 22(12):1913–1921, 2009.
- [96] Kaitlyn M Gayvert, Neel S Madhukar, and Olivier Elemento. A data-driven approach to predicting successes and failures of clinical trials. *Cell chemical biology*, 23(10):1294–1301, 2016.

- [97] Yushi Hu, Hang Hua, Zhengyuan Yang, Weijia Shi, Noah A Smith, and Jiebo Luo. Prompt-cap: Prompt-guided image captioning for vqa with gpt-3. In *Proceedings of the IEEE/CVF International Conference on Computer Vision*, pages 2963–2975, 2023.
- [98] Woojeong Jin, Yu Cheng, Yelong Shen, Weizhu Chen, and Xiang Ren. A good prompt is worth millions of parameters: Low-resource prompt-based learning for vision-language models. *arXiv preprint arXiv:2110.08484*, 2021.
- [99] Yunshi Lan, Xiang Li, Xin Liu, Yang Li, Wei Qin, and Weining Qian. Improving zero-shot visual question answering via large language models with reasoning question prompts. In *Proceedings of the 31st ACM International Conference on Multimedia*, pages 4389–4400, 2023.
- [100] Linjie Li, Jie Lei, Zhe Gan, and Jingjing Liu. Adversarial vqa: A new benchmark for evaluating the robustness of vqa models. In *Proceedings of the IEEE/CVF International Conference on Computer Vision*, pages 2042–2051, 2021.
- [101] Oscar Mañas, Benno Krojer, and Aishwarya Agrawal. Improving automatic vqa evaluation using large language models. In *Proceedings of the AAAI Conference on Artificial Intelligence*, volume 38, pages 4171–4179, 2024.
- [102] National Center for Biotechnology Information. PubChem Compound Summary for CID 94022. <https://pubchem.ncbi.nlm.nih.gov/compound/94022>, 2025. Accessed: 2025-05-13.
- [103] G Richard Bickerton, Gaia V Paolini, Jérémy Besnard, Sorel Muresan, and Andrew L Hopkins. Quantifying the chemical beauty of drugs. *Nature chemistry*, 4(2):90–98, 2012.
- [104] Peter Ertl and Ansgar Schuffenhauer. Estimation of synthetic accessibility score of drug-like molecules based on molecular complexity and fragment contributions. *Journal of cheminformatics*, 1:1–11, 2009.
- [105] Christopher A Lipinski, Franco Lombardo, Beryl W Dominy, and Paul J Feeney. Experimental and computational approaches to estimate solubility and permeability in drug discovery and development settings. *Advanced drug delivery reviews*, 64:4–17, 2012.
- [106] David Rogers and Mathew Hahn. Extended-connectivity fingerprints. *Journal of chemical information and modeling*, 50(5):742–754, 2010.
- [107] Aaron Jaech and Adam et al. Kalai. Openai o1 system card. *arXiv preprint arXiv:2412.16720*, 2024.
- [108] OpenAI. Introducing gpt-4.1 in the api. <https://openai.com/index/gpt-4-1/>, 2025. Accessed: 2025-05-05.
- [109] xAI. Grok 3 beta — the age of reasoning agents. <https://x.ai/news/grok-3>, 2025. Accessed: May 5, 2025.
- [110] Zhipu AI. Glm-4v-plus: A multimodal large language model. <https://open.bigmodel.cn/dev/howuse/glm-4v>, 2024. Accessed: May 5, 2025.
- [111] Kimi Team, Angang Du, and Bohong et al. Yin. Kimi-vl technical report. *arXiv preprint arXiv:2504.07491*, 2025.
- [112] Tencent Hunyuan Team. Hunyuan-vision: Tencent’s multimodal vision-language model. <https://cloud.tencent.com/document/product/1729/104753>, 2024. Accessed: 2025-05-07.
- [113] Zhiyu Wu and Xiaokang et al. Chen. Deepseek-vl2: Mixture-of-experts vision-language models for advanced multimodal understanding. *arXiv preprint arXiv:2412.10302*, 2024.
- [114] Bo Li and Yuanhan et al. Zhang. Llava-onevision: Easy visual task transfer. *arXiv preprint arXiv:2408.03326*, 2024.

A Prompt Template Example for Tox21 Tasks

In this appendix, we provide an illustrative template example to complement the mechanism-aware prompt annotation pipeline introduced in Section 3.2. The included configuration consists of the base prompt template that defines the MLLM role, repair objectives, formatting constraints shown in Fig. 6, and task-level annotation specific to the Tox21 dataset shown in Fig. 7. Furthermore, we include 12 subtask-specific prompt fragments corresponding to the individual endpoints within the Tox21 benchmark (T1–T12), as shown in Table 5, each reflecting the unique toxicity mechanism it represents. This example is a reference for understanding how prompts are hierarchically composed and adapted for different toxicity contexts.

role_definition
You are a specialized medicinal chemistry expert focused on structural optimization of small molecules to reduce toxicity while maintaining pharmacological efficacy.

task_overview
Given a molecule (presented as both SMILES string and molecular structure image) and a specified toxicity repair task, suggest structural modifications to reduce the specified toxicity while preserving or improving drug-likeness properties.

image_integration
"purpose": "The molecular structure image provides critical spatial and conformational information that complements the SMILES representation.",
"usage_guidelines":
["Analyze structural features visible in the 2D representation that may contribute to toxicity",
"Observe spatial arrangements of functional groups that may interact with biological targets",
"Identify structural alerts and toxicophores based on their visual presentation",
"Consider how conformational aspects visible in the image might influence biological interactions"]

secondary_constraints
"Minimize Lipinski rule violations", "Maintain LogP within <5", "Maintain low synthetic accessibility (SAS score)", "Preserve sufficient structural similarity to the original molecule",

modification_principles
"Prefer removal or replacement of known toxicophores", "Ensure all generated SMILES are chemically valid and syntactically correct", "Ensure that all generated SMILES are syntactically correct and must be valid according to RDKit parsing", "All generated SMILES must be kekulizable and chemically valid according to RDKit; avoid valence issues, non-aromatic aromatic rings, and ambiguous bond notations."

thought_process
"First, analyze both the SMILES notation and molecular image to identify structural features associated with the specified toxicity", "Second, consider multiple potential modifications, weighing their impact on toxicity vs. pharmacological properties", "Third, prioritize modifications that specifically address the toxicity mechanism while maintaining core pharmacophores", "Fourth, evaluate the chemical feasibility and synthetic accessibility of each modification", "Fifth, visualize how the proposed modifications would appear structurally compared to the original molecule", "Finally, select the most promising candidates that balance toxicity reduction with preservation of drug properties"

output_format
"structure": "MODIFIED_SMILES: smiles1;smiles2;smiles3",
"notes":
["Strictly follow this exact format with the keyword 'MODIFIED_SMILES:' followed by semicolon-separated SMILES strings", "Include 3 modified SMILES only", "Do not include any explanations, rationales or other text - ONLY provide the SMILES", "If no feasible modification is found, output: 'MODIFIED_SMILES: none'", "All SMILES must be kekulizable by RDKit (i.e., no SMILES that trigger 'Can't kekulize mol' errors); avoid ambiguous aromatic systems or invalid bond syntax.", "No bullet points, no line breaks, just pure SMILES separated by semicolons", "Example correct format: 'MODIFIED_SMILES: C1CCCCC1;C1CCCCC1'"]

Figure 6: Overall prompt design for detoxification tasks using MLLMs.

task_name
tox21

task_description
Compound with Tox21-related toxicity pathways

subtasks
"NR_AR":
{"description": "Androgen Receptor interaction",
"instruction": "Given molecule with the provided SMILES and molecular structure image, which interacts with the androgen receptor (NR-AR). Please modify its structure to reduce its binding affinity to the androgen receptor while maintaining its primary pharmacophore. Specifically, focus on modifying structural elements that may interact with the androgen receptor binding site, such as steroid-like scaffolds or specific hydrogen bond donor/acceptor groups."},
"NR_AR_LBD":
{"description": "Androgen Receptor Ligand Binding Domain interaction",
"instruction": "Given molecule with the provided SMILES and molecular structure image, which interacts with the androgen receptor ligand binding domain (NR-AR-LBD). Please design structural modifications to decrease its binding affinity to AR-LBD while maintaining its original drug-like properties. Pay special attention to: avoid modifications that significantly increase lipophilicity, and consider introducing steric hindrance to interfere with receptor binding."},
.....
"NR_AhR":
{"description": "Aryl hydrocarbon Receptor activation",
"instruction": "Given molecule with the provided SMILES and molecular structure image, which is an aryl hydrocarbon receptor (AhR) agonist. Please modify its structure to reduce its ability to activate AhR while preserving its main pharmacological properties. The aryl hydrocarbon receptor particularly interacts with planar aromatic structures, so consider altering the molecular coplanarity or modifying key aromatic ring systems."},

output_format
Please propose structural modifications that specifically address the toxicity mechanism identified in the Tox21 assay while preserving the core pharmacological properties of the molecule.

Figure 7: Task prompt design for detoxification tasks of Tox21 using MLLMs.

B Tox21 Subtask Definitions and Toxicity Mechanisms

Table 5 overviews the 12 subtasks from the Tox21 dataset, listing each task’s identifier (T1–T12), subtask name, and the corresponding toxicity mechanism. These subtasks cover many biological pathways, including oxidative stress, DNA damage, endocrine receptor activation, and gene expression regulation. In our evaluation framework, each subtask is assessed independently to systematically evaluate the capacity of MLLMs to understand and address diverse mechanisms of molecular toxicity.

Table 5: List of Tox21 Subtasks and Corresponding Toxicity Mechanisms.

Task ID	Subtask Name	Toxicity Mechanism
T1	Tox21_SR_ARE	Oxidative stress response via Antioxidant Response Element (ARE)
T2	Tox21_SR_p53	Genotoxic stress-induced activation of p53 tumor suppressor pathway
T3	Tox21_NR_Aromatase	Endocrine disruption via inhibition of aromatase enzyme
T4	Tox21_SR_ATAD5	DNA replication stress signaling through ATAD5 gene expression
T5	Tox21_NR_ER_LBD	Estrogen receptor Ligand-binding Domain (ER-LBD) activation
T6	Tox21_SR_HSE	Heat shock response through Heat Shock Element (HSE) signaling
T7	Tox21_NR_AR	Androgen receptor (AR) activation and antagonism
T8	Tox21_NR_PPAR- γ	Modulation of Peroxisome Proliferator-Activated Receptor- γ (PPAR- γ)
T9	Tox21_NR_ER	Full-length Estrogen Receptor (ER) activation
T10	Tox21_SR_MMP	Mismatch repair signaling (MMP-related genotoxicity)
T11	Tox21_NR_AhR	Aryl Hydrocarbon Receptor (AhR) binding and activation
T12	Tox21_NR_AR_LBD	Ligand-binding Domain modulation of Androgen Receptor (AR-LBD)

C ToxCast Subtask Definitions and Toxicity Mechanisms

Table 6 lists 10 representative subtasks selected from the ToxCast dataset, encompassing diverse toxicity pathways such as mitochondrial dysfunction, immunosuppression, developmental toxicity, metal response, GPCR activation, and neurotoxicity. These tasks extend the evaluation beyond Tox21 and assess the generalization ability of MLLMs in handling complex and varied molecular toxicity mechanisms. Each subtask is evaluated independently within the ToxiEval framework to ensure granularity and interpretability.

Table 6: List of ToxCast Subtasks and Corresponding Toxicity Mechanisms.

Task ID	Subtask Name	Toxicity Mechanism
T1	ToxCast_APR_HepG2_MitoMass_24h_dn	Mitochondrial toxicity in HepG2 cells (24h exposure)
T2	ToxCast_BSK_3C_ICAM1_down	Suppression of ICAM1 expression in immune cell model (inflammation)
T3	ToxCast_Tanguay_ZF_120hpf_TR_up	Zebrafish developmental response at 120 hpf (transcriptional activation)
T4	ToxCast_ATG_M_32_CIS_dn	Downregulation of CIS gene (cell proliferation inhibition)
T5	ToxCast_ATG_ROR- γ _TRANS_up	Activation of Retinoic Acid Receptor-related Orphan Receptor- γ (ROR- γ)
T6	ToxCast_TOX21_p53_BLA_p3_ch2	Genotoxic response via p53 reporter activation
T7	ToxCast_BSK_3C_MCP1_down	Immunosuppression via MCP1 downregulation in BioMAP assay
T8	ToxCast_ATG_MRE_CIS_up	Activation of Metal-Responsive Element (MRE) pathway
T9	ToxCast_NVS_GPCR_gLTB4	GPCR pathway activation via Leukotriene B4 receptor binding
T10	ToxCast_NVS_ENZ_hAChE	Inhibition of human acetylcholinesterase (neurotoxicity marker)

D Symbolic Notation for Mechanism-Aware Prompt Annotation Pipeline

Table 7 summarizes the symbolic notations used throughout the mechanism-aware prompt annotation pipeline described in Subsection 3.2. These symbols represent the key components of the toxicity repair process, including task identifiers, molecule inputs, 2D structural images, hierarchical prompt components, and MLLM-generated outputs.

E Mechanism-Aware Prompt Annotation Pipeline

Algorithm 1 presents the mechanism-aware prompt annotation pipeline for generating molecule-specific repair instructions in the ToxiMol benchmark. Given a toxicity repair task \mathcal{T} , a set of toxicity-positive molecules \mathcal{S}^{raw} , and corresponding structure images $\{\text{IMG}_i\}$, the system first loads a shared base prompt $\mathcal{P}_{\text{base}}$ and task-level annotations $\mathcal{P}_{\text{task}}$. For tasks with subtask granularity, an additional subtask annotation $\mathcal{P}_{\text{subtask}}$ is injected per molecule based on its inferred category.

Table 7: **Symbol Definitions for Mechanism-Aware Prompt Annotation Pipeline.**

Symbol	Definition
\mathcal{T}	Toxicity repair task identifier (e.g., AMES, DILI, hERG).
$\mathcal{S}^{\text{raw}} = \{\text{SMILES}_i^{\text{raw}}\}_{i=1}^n$	Set of toxicity-positive SMILES strings requiring repair.
IMG_i	2D molecular structure image associated with $\text{SMILES}_i^{\text{raw}}$, rendered via RDKit.
$\mathcal{P}_{\text{base}}$	Base prompt template encoding MLLM role, objectives, and formatting rules.
$\mathcal{P}_{\text{task}}$	Task-level annotation describing toxicity mechanism and optimization focus.
$\mathcal{P}_{\text{subtask}}$	Subtask-level annotation for fine-grained tasks (e.g., specific Tox21 endpoints).
\mathcal{P}_i	Final prompt for molecule i , including template, annotations, SMILES, and image.
\mathcal{M}	MLLMs queried for toxicity repair.
$\mathcal{S}_i^{\text{rep}} = \{\text{SMILES}_i^{\text{rep}(k)}\}_{k=1}^3$	Candidate repaired SMILES outputs generated by \mathcal{M} for molecule i .
\mathcal{S}^{rep}	Final set of all generated candidate molecules across the input batch.

Algorithm 1: Mechanism-Aware Prompt Annotation Pipeline

Input: Toxicity repair task name \mathcal{T} ; toxicity-positive molecule set $\mathcal{S}^{\text{raw}} = \{\text{SMILES}_i^{\text{raw}}\}_{i=1}^n$; corresponding images $\{\text{IMG}_i\}_{i=1}^n$; MLLM model \mathcal{M}
Output: Repaired molecule candidates \mathcal{S}^{rep}

- 1 Initialize empty output set: $\mathcal{S}^{\text{rep}} \leftarrow \emptyset$;
- 2 Load base template: $\mathcal{P}_{\text{base}} \leftarrow \text{LoadBasePrompt}()$;
- 3 Load task-level annotations: $\mathcal{P}_{\text{task}} \leftarrow \text{LoadTaskAnnotation}(\mathcal{T})$;
- 4 **foreach** $i = 1$ **to** n **do**
- 5 **if** \mathcal{T} **has subtask** **then**
- 6 Identify subtask: $t_i \leftarrow \text{InferSubtask}(\text{SMILES}_i^{\text{raw}})$;
- 7 Load subtask annotations: $\mathcal{P}_{\text{subtask}} \leftarrow \text{LoadSubtaskAnnotation}(t_i)$;
- 8 **else**
- 9 $\mathcal{P}_{\text{subtask}} \leftarrow \emptyset$;
- 10 **end**
- 11 Assemble full prompt: $\mathcal{P}_i \leftarrow \text{Assemble}(\mathcal{P}_{\text{base}}, \mathcal{P}_{\text{task}}, \mathcal{P}_{\text{subtask}}, \text{SMILES}_i^{\text{raw}}, \text{IMG}_i)$;
- 12 Inject reasoning chain: $\mathcal{P}_i \leftarrow \mathcal{P}_i + \text{InsertCoTReasoningSteps}()$;
- 13 Inject few-shot examples (optional): $\mathcal{P}_i \leftarrow \mathcal{P}_i + \text{InsertFewShotExamples}()$;
- 14 Append output constraints: $\mathcal{P}_i \leftarrow \mathcal{P}_i + \text{InsertOutputFormatSpec}()$;
- 15 Query MLLM: $\mathcal{S}_i^{\text{rep}} \leftarrow \mathcal{M}(\mathcal{P}_i)$;
- 16 Add to output: $\mathcal{S}^{\text{rep}} \leftarrow \mathcal{S}^{\text{rep}} \cup \mathcal{S}_i^{\text{rep}}$;
- 17 **end**
- 18 **return** \mathcal{S}^{rep} ;

Each complete prompt \mathcal{P}_i is assembled by integrating molecular SMILES, 2D image features, and mechanism-specific constraints. The prompt is then augmented with optional Chain-of-Thought (CoT) reasoning steps and few-shot exemplars to enhance model interpretability and generalization. Finally, strict output format constraints are appended to ensure syntactic and chemical validity. The multimodal prompt \mathcal{P}_i is passed to the MLLMs \mathcal{M} to generate candidate repaired molecules $\mathcal{S}_i^{\text{rep}}$, which are collected across all samples to produce the final output set \mathcal{S}^{rep} .

F Intuitive Explanation of ToxiEval Evaluation Metrics

This section provides conceptual explanations for the five evaluation metrics used in the ToxiEval framework, helping readers understand their semantic meanings and practical relevance in the context of molecular toxicity repair.

Quantitative Estimate of Drug-likeness (QED, \mathcal{Q}). QED quantifies how closely a molecule resembles typical drug-like compounds. A candidate molecule must retain adequate drug-likeness even after successful toxicity reduction to be considered pharmaceutically viable. The QED score ranges from 0 to 1, with higher values indicating better alignment with known drug-like properties. It integrates multiple molecular features, including Molecular Weight (MW), Partition coefficient (logP), and the number of Hydrogen Bond Donors (HBD) and Acceptors (HBA), among others. A significantly lower QED score in a repaired molecule \mathcal{S}_i compared to its toxic precursor $\mathcal{S}_i^{\text{raw}}$ may suggest a loss of drug development potential, despite successful toxicity mitigation.

Lipinski’s Rule of Five (RO5, \mathcal{V}_{ro5}). RO5 is a widely adopted heuristic for evaluating the oral bioavailability of small molecules. It defines four property-based constraints: $\text{MW} \leq 500$ Da, $\log\text{P} \leq 5$, $\text{HBD} \leq 5$, and $\text{HBA} \leq 10$. A molecule that violates more than one of these conditions (i.e., $\mathcal{V}_{\text{ro5}} > 1$) is generally considered less likely to exhibit favorable oral absorption. Structural modifications during toxicity repair may increase molecular weight or lipophilicity, resulting in elevated RO5 violations. Although originally designed for oral drugs, RO5 remains a valuable indicator of drug-likeness and structural feasibility across broader chemical design spaces.

Synthetic Accessibility Score (SAS, \mathcal{S}_{sas}). SAS estimates how easily a molecule can be synthesized in a laboratory setting. Scores range from 1 (very easy) to 10 (very difficult). High scores reflect complex ring systems, rare substructures, or unstable fragments that hinder synthesis. In ToxiEval, we use \mathcal{S}_{sas} to assess whether a generated candidate is practically accessible, thereby bridging the gap between virtual optimization and real-world chemical feasibility.

Structural Similarity (SS, \mathcal{S}_{sim}). To ensure that the semantic identity of a molecule is preserved during repair, ToxiEval computes the Tanimoto similarity between the repaired molecule and the original toxic precursor. Let \mathbf{f}^{raw} and $\mathbf{f}^{(i)}$ denote the fingerprint vectors of $\mathcal{S}_i^{\text{raw}}$ and its repaired version s_i , respectively. The Tanimoto similarity is defined as:

$$\mathcal{S}_{\text{sim}} = \frac{|\mathbf{f}^{\text{raw}} \cap \mathbf{f}^{(i)}|}{|\mathbf{f}^{\text{raw}} \cup \mathbf{f}^{(i)}|}.$$

Here, Extended Connectivity Fingerprints (e.g., ECFP6) are typically used. Higher values of \mathcal{S}_{sim} indicate that the core scaffold remains intact, implying a mild structural adjustment. Conversely, low similarity implies substantial structural changes that may compromise molecular identity or original pharmacophores.

G Symbol Definitions for ToxiEval Evaluation Framework

Table 8 defines the notations used in the ToxiEval evaluation framework described in Section 3.3. These symbols cover the key components of the multi-criteria decision process, including the structure of candidate sets, task-aware safety prediction, cheminformatics-derived molecular properties, and threshold-based decision variables.

Table 8: Symbol Definitions for the ToxiEval Evaluation Framework.

Symbol	Definition
$\text{SMILES}_i^{\text{raw}}$	Original toxicity-positive molecule requiring repair.
$\mathcal{S}_i^{\text{rep}} = \{\text{SMILES}_i^{\text{rep}(1)}, \text{SMILES}_i^{\text{rep}(2)}, \text{SMILES}_i^{\text{rep}(3)}\}$	Candidate repaired molecules generated by the MLLM for input i .
$s \in \mathcal{S}_i^{\text{rep}}$	A single candidate molecule from the repaired set.
\mathcal{T}	Toxicity repair task identifier (e.g., AMES, DILI, hERG, LD50).
\mathcal{G}_{tox}	Toxicity prediction model used for safety scoring (e.g., TxGemma-Predict).
$\mathcal{S}_{\text{safe}}$	Safety score of s based on task \mathcal{T} (binary or normalized).
\mathcal{Q}	QED (Quantitative Estimate of Drug-likeness) score of candidate s , in $[0, 1]$.
\mathcal{S}_{sas}	Synthetic Accessibility Score of candidate s , in $[1, 10]$ (lower is better).
\mathcal{V}_{ro5}	Number of violations of Lipinski’s Rule of Five by candidate s .
\mathcal{S}_{sim}	Tanimoto similarity between candidate s and original molecule $\text{SMILES}_i^{\text{raw}}$.
\mathcal{C}^*	Set of evaluation thresholds for all criteria (e.g., $\mathcal{Q} \geq 0.5$, $\mathcal{S}_{\text{sas}} \leq 6$).
$\text{success}_i \in \{0, 1\}$	Boolean label indicating whether any $s \in \mathcal{S}_i^{\text{rep}}$ satisfies all criteria.

H ToxiEval Algorithm: Multi-Criteria Decision Protocol for Molecular Toxicity Repair

Algorithm 2 presents the ToxiEval evaluation pipeline to determine whether a candidate molecule satisfies the multi-criteria toxicity repair constraints defined in Section 3.3. Given an original molecule $\text{SMILES}_i^{\text{raw}}$ and a set of candidate repairs $\mathcal{S}_i^{\text{rep}}$ generated by an MLLM, the system first checks structural validity using RDKit. For valid candidates, it invokes the toxicity predictor \mathcal{G}_{tox} to assign a safety score, either through label classification or normalized LD50 regression. Additional properties—including Drug-Likeness (QED), Synthetic Accessibility Score (SAS), Lipinski’s Rule of Five (RO5), and Structural Similarity (SS)—are computed using cheminformatics tools. The

evaluation adopts a strict conjunctive decision protocol: a candidate is deemed successful only if all criteria pass their respective thresholds. If any candidate in $\mathcal{S}_i^{\text{rep}}$ passes, the molecule is labeled as successfully repaired. This pipeline ensures rigorous, fine-grained assessment of molecular repair quality under realistic multi-objective constraints.

Algorithm 2: ToxiEval: Multi-Criteria Evaluation Pipeline for Toxicity Repair

Input: Candidate set $\mathcal{S}_i^{\text{rep}} = \{\text{SMILES}_i^{\text{rep}(1)}, \text{SMILES}_i^{\text{rep}(2)}, \text{SMILES}_i^{\text{rep}(3)}\}$; original molecule $\text{SMILES}_i^{\text{raw}}$; task identifier \mathcal{T} ; toxicity predictor \mathcal{G}_{tox} ; threshold set \mathcal{C}^* .

Output: Repair success label $\text{success}_i \in \{0, 1\}$

```

1 successi ← 0;
2 foreach s ∈ Sirep do
3     /* Step 1: Structure validity check */
4     if IsValid ← RDKitParse(s) = False then
5         continue;
6     /* Step 2: Safety scoring via toxicity prediction */
7     if T = LD50 then
8         vtox ← Gtox(s);
9         Ssafe ← Normalize(vtox, [0, 1000]);
10        passedsafe ← Ssafe > 0.5;
11    else
12        ytox ← Gtox(s);
13        passedsafe ← (ytox = A);
14    /* Step 3: Compute molecular evaluation metrics */
15    Q ← ComputeQED(s);
16    Ssas ← ComputeSAS(s);
17    Vro5 ← CountRO5Violations(s);
18    Ssim ← TanimotoSimilarity(s, SMILESiraw);
19    /* Step 4: Apply conjunctive success decision */
20    if passedsafe and Q ≥ Cqed* and Ssas ≤ Csas* and Vro5 ≤ Cro5* and Ssim ≥ Csim* then
21        successi ← 1; break;
22 return successi;

```

I Success Rates of Each Model on the 12 Sub-Tasks of Tox21

Table 9 presents the success rates of various MLLMs across the 12 subtasks defined in the Tox21 benchmark. Each model is evaluated independently per subtask based on a strict structure-level success criterion, reflecting its capacity to generate detoxified molecular structures that align with the desired toxicity mechanism. The table highlights significant performance variance across models and subtasks, with closed-source models generally outperforming open-source counterparts. Notably, tasks involving nuclear receptor activation (e.g., ER, AR) exhibit higher success rates, suggesting their relatively more explicit structure-to-function mappings. The corresponding subtask identifiers (T1–T12), task names and associated toxicity mechanisms are summarized in Table 5.

J Success Rates of Each Model on the 10 Selected Sub-Tasks of ToxCast

Table 10 reports model-level success rates on a broader and mechanistically diverse set of 10 subtasks selected from the ToxCast dataset. These subtasks involve toxicity mechanisms such as mitochondrial stress, immune suppression, GPCR modulation, and neurotoxicity. Compared to Tox21, the overall success rates are lower and more variable, reflecting the increased complexity and heterogeneity of the underlying biological pathways. The results demonstrate MLLMs’ challenge in generalizing across domains while revealing specific models’ robustness under broader task definitions. The corresponding subtask identifiers (T1–T10), task names, and associated toxicity mechanisms are summarized in Table 6.

Table 9: Success Rates of Each Model on the 12 Sub-Tasks of Tox21.

Models	T1	T2	T3	T4	T5	T6	T7	T8	T9	T10	T11	T12
Close Source MLLMs												
GPT-o4-mini [1]	60.0	80.0	100.0	60.0	100.0	80.0	80.0	60.0	80.0	80.0	40.0	60.0
GPT-o3 [1]	60.0	80.0	100.0	20.0	80.0	80.0	80.0	80.0	80.0	60.0	100.0	80.0
GPT-o1 [107]	40.0	60.0	60.0	20.0	100.0	100.0	80.0	80.0	100.0	80.0	40.0	80.0
GPT-4.1 [108]	60.0	80.0	80.0	20.0	80.0	60.0	80.0	80.0	100.0	60.0	0.0	60.0
GPT-4o [55]	40.0	60.0	60.0	20.0	100.0	80.0	80.0	60.0	100.0	60.0	60.0	60.0
Claude-3.7 Sonnet Thinking [2]	20.0	60.0	100.0	40.0	60.0	100.0	100.0	60.0	80.0	80.0	0.0	60.0
Claude-3.7 Sonnet [2]	40.0	60.0	60.0	20.0	100.0	100.0	80.0	80.0	100.0	80.0	40.0	80.0
Claude-3 Opus [56]	60.0	80.0	60.0	20.0	80.0	60.0	80.0	60.0	100.0	80.0	40.0	80.0
Gemini-2.5 pro-exp [60]	20.0	80.0	100.0	20.0	80.0	60.0	80.0	80.0	100.0	80.0	40.0	80.0
Gemini-2.0 flash-thinking-exp [59]	40.0	80.0	60.0	40.0	40.0	100.0	80.0	60.0	100.0	80.0	20.0	20.0
Gemini-1.5-pro [58]	40.0	80.0	80.0	20.0	80.0	60.0	80.0	60.0	80.0	60.0	20.0	80.0
Grok-2-vision [109]	40.0	80.0	60.0	20.0	60.0	40.0	80.0	60.0	100.0	40.0	40.0	60.0
GLM-4v-plus [110]	20.0	20.0	40.0	20.0	60.0	40.0	80.0	60.0	60.0	60.0	60.0	60.0
Moonshot-v1-128k-vision [111]	0.0	40.0	40.0	20.0	80.0	40.0	60.0	60.0	100.0	60.0	20.0	80.0
hunyuan-vision [112]	0.0	40.0	20.0	20.0	60.0	0.0	20.0	60.0	80.0	60.0	20.0	60.0
Open Source MLLMs												
InternVL3.0-8B [14]	20.0	0.0	0.0	20.0	80.0	20.0	20.0	0.0	20.0	0.0	0.0	40.0
InternVL3.0-14B [3]	20.0	60.0	40.0	20.0	60.0	60.0	60.0	40.0	60.0	40.0	40.0	40.0
InternVL3.0-38B [3]	20.0	60.0	80.0	20.0	60.0	20.0	60.0	0.0	80.0	60.0	20.0	60.0
InternVL3.0-78B [69]	0.0	60.0	40.0	20.0	80.0	80.0	80.0	20.0	60.0	80.0	20.0	60.0
Qwen2.5-VL-7B-Instruct [4]	0.0	40.0	0.0	20.0	20.0	20.0	0.0	0.0	0.0	0.0	40.0	40.0
Qwen2.5-VL-32B-Instruct [4]	60.0	60.0	80.0	20.0	80.0	0.0	40.0	80.0	80.0	20.0	60.0	60.0
Qwen2.5-VL-72B-Instruct [4]	60.0	40.0	40.0	0.0	80.0	40.0	80.0	80.0	80.0	40.0	80.0	80.0
DeepSeek-VL2-tiny [113]	0.0	60.0	40.0	20.0	60.0	40.0	60.0	60.0	60.0	60.0	20.0	60.0
DeepSeek-VL2-small [113]	0.0	40.0	40.0	40.0	80.0	60.0	80.0	60.0	60.0	60.0	20.0	60.0
DeepSeek-VL2 [113]	0.0	40.0	40.0	20.0	60.0	40.0	80.0	60.0	40.0	80.0	20.0	60.0
LLaVA-OneVision-7B [114]	20.0	60.0	40.0	20.0	80.0	80.0	80.0	40.0	60.0	60.0	20.0	60.0
LLaVA-OneVision-72B [114]	40.0	80.0	60.0	20.0	40.0	40.0	60.0	60.0	60.0	60.0	60.0	60.0
Average Success Rate	28.1	57.0	56.3	23.0	71.9	56.3	68.1	55.6	74.8	57.8	35.6	62.2

K Analysis of hERG-Related Tasks

In the previous experiments 4.2, we observed significant differences in success rates across the three hERG-related tasks (hERG, hERG_C, and hERG_K) when evaluating model-generated repair candidates. We designed the following ablation study to investigate further the two hypothesized factors—prompt formulation differences and discrepancies in TxGemma-Predict [38] evaluation standards. Specifically, we standardized the prompt across all three tasks using the hERG_C template, which exhibits the most balanced and well-structured format regarding structural description, task instruction, and in-context examples. Claude-3.7 Sonnet [2], the best-performing model, generated repair candidates on a fixed test set. These candidates were then evaluated using the ToxiEval framework. The results are summarized in Table 11.

The experimental results indicate that standardizing all prompts to the hERG_C format effectively improves the success rate on the original hERG task, increasing eight percentage points. This confirms that prompt formulation style significantly influences model comprehension and response quality. However, we also observed a slight decrease in the success rates of hERG_C and hERG_K under the unified prompt condition, suggesting that even with a fixed test set, MLLM generation quality may still exhibit some variability.

More importantly, despite using the same prompt, the success rate on hERG remained substantially lower than that on hERG_C and hERG_K. This further supports our hypothesis regarding endpoint semantic inconsistencies in the TxGemma-Predict evaluation mechanism. In toxicological contexts, the term “block hERG” is typically interpreted as a stricter form of “inhibit hERG,” implying that the model must identify more pronounced structural toxicity features—thereby increasing task difficulty and reducing the success rate.

Table 10: Success Rates of Each Model on the 10 Selected Sub-Tasks of ToxCast.

Models	T1	T2	T3	T4	T5	T6	T7	T8	T9	T10
Close Source MLLMs										
GPT-o4-mini [1]	60.0	40.0	100.0	80.0	80.0	40.0	100.0	40.0	60.0	40.0
GPT-o3 [1]	60.0	60.0	80.0	80.0	80.0	40.0	80.0	80.0	60.0	40.0
GPT-o1 [107]	60.0	20.0	80.0	40.0	60.0	20.0	100.0	60.0	60.0	60.0
GPT-4.1 [108]	60.0	40.0	100.0	40.0	60.0	100.0	100.0	80.0	80.0	60.0
GPT-4o [55]	60.0	40.0	100.0	80.0	20.0	20.0	100.0	60.0	60.0	20.0
Claude-3.7 Sonnet Thinking [2]	80.0	40.0	100.0	80.0	60.0	20.0	100.0	80.0	60.0	60.0
Claude-3.7 Sonnet [2]	60.0	60.0	100.0	80.0	40.0	40.0	100.0	80.0	60.0	60.0
Claude-3 Opus [56]	60.0	60.0	100.0	60.0	40.0	40.0	80.0	80.0	40.0	60.0
Gemini-2.5 pro-exp [60]	60.0	40.0	100.0	60.0	80.0	20.0	100.0	60.0	60.0	40.0
Gemini-2.0 flash-thinking-exp [59]	20.0	20.0	100.0	60.0	40.0	40.0	80.0	60.0	80.0	40.0
Gemini-1.5-pro [58]	80.0	40.0	100.0	60.0	60.0	20.0	80.0	60.0	60.0	40.0
Grok-2-vision [109]	60.0	60.0	80.0	40.0	20.0	60.0	100.0	60.0	40.0	40.0
GLM-4v-plus [110]	40.0	20.0	80.0	40.0	20.0	20.0	80.0	40.0	40.0	40.0
Moonshot-v1-128k-vision [111]	40.0	60.0	80.0	40.0	20.0	40.0	100.0	40.0	60.0	20.0
hunyuan-vision [112]	60.0	40.0	60.0	40.0	0.0	20.0	100.0	60.0	40.0	40.0
Open Source MLLMs										
InternVL3.0-8B [14]	40.0	20.0	40.0	60.0	0.0	0.0	20.0	20.0	60.0	40.0
InternVL3.0-14B [3]	80.0	40.0	80.0	20.0	80.0	20.0	80.0	40.0	80.0	20.0
InternVL3.0-38B [3]	60.0	40.0	40.0	20.0	40.0	40.0	60.0	20.0	60.0	40.0
InternVL3.0-78B [69]	60.0	40.0	80.0	40.0	20.0	60.0	80.0	60.0	60.0	40.0
Qwen2.5-VL-7B-Inst. [4]	0.0	0.0	0.0	0.0	0.0	0.0	0.0	0.0	0.0	40.0
Qwen2.5-VL-32B-Inst. [4]	60.0	40.0	100.0	20.0	40.0	60.0	80.0	40.0	80.0	20.0
Qwen2.5-VL-72B-Inst. [4]	60.0	20.0	80.0	20.0	0.0	40.0	80.0	40.0	40.0	40.0
DeepSeek-VL2-tiny [113]	20.0	0.0	60.0	20.0	20.0	20.0	80.0	60.0	40.0	40.0
DeepSeek-VL2-small [113]	60.0	0.0	80.0	40.0	20.0	20.0	80.0	60.0	60.0	40.0
DeepSeek-VL2 [113]	60.0	20.0	60.0	20.0	20.0	40.0	80.0	40.0	20.0	20.0
LLaVA-OneVision-7B [114]	60.0	20.0	60.0	0.0	20.0	20.0	80.0	60.0	40.0	40.0
LLaVA-OneVision-72B [114]	40.0	40.0	40.0	0.0	20.0	40.0	80.0	80.0	40.0	20.0
Average Success Rate	54.1	33.3	77.0	42.2	37.0	31.9	80.7	54.8	54.1	38.5

Table 11: Comparison of success rates (%) on hERG-related tasks using the original versus unified prompt templates.

Prompt Template	hERG	hERG _C	hERG _K
Original	8.0	68.0	50.0
Unified	16.0	60.0	40.0

L TxGemma-Predict Model Selection

In the ToxiEval framework, the toxicity endpoint classification module is powered by the TxGemma-Predict model family [38], which includes three versions with different parameter scales: 2B, 9B, and 27B. We adopted the 9B version in our main experiments to balance prediction accuracy and computational cost. To further analyze the impact of the evaluation model scale on toxicity repair outcomes, we compared the 2B and 27B variants, representing the most minor and most significant models in the TxGemma series. All other settings were held constant, and the candidate molecules generated by Claude-3.7 Sonnet [2] were used as inputs. The comparison of success rates under different TxGemma versions is presented in Table 12.

Table 12: Task-level success rates (%) of the TxGemma-Predict model family on the toxicity-repair benchmark.

Model	LD50	hERG _C	Carc _L	Tox21	AMES	ToxCast	ClinTox	DILI	hERG _K	hERG	SkinRx _i	Overall
TxGemma-Predict-2B	0.0	76.0	30.0	70.0	22.0	64.0	62.0	8.0	46.0	8.0	6.0	36.3
TxGemma-Predict-9B	4.0	68.0	28.0	70.0	34.0	68.0	56.0	8.0	50.0	8.0	2.0	36.6
TxGemma-Predict-27B	2.0	76.0	32.0	68.3	34.0	70.0	52.0	14.0	54.0	22.0	28.0	41.6

Table 13: **Toxicity Repair Valid Rates (%)**. hERGC, hER GK, and Carc_L refer to the hERG_Central, hERG_Karim, and Carcinogens tasks, respectively. SkinRxn denotes the SkinReaction task. Claude-3.7 Sonnet (20250219), Claude-3 Opus (20240229), and Gemini-2.5 pro-exp (20250325) indicate the specific model versions used for evaluation.

Models	LD50	hERGC	Carc _L	Tox21	AMES	ToxCast	ClinTox	DILI	hER GK	hERG	SkinRxn	Overall
Close Source MLLMs												
GPT-o4-mini [1]	97.3	69.3	89.3	95.6	82.7	92.0	90.7	91.3	90.7	89.3	96.0	89.6
GPT-o3 [1]	97.3	66.0	92.7	95.0	92.0	93.3	88.0	89.3	92.0	93.3	97.3	90.7
GPT-o1 [107]	84.7	87.3	74.0	82.8	74.0	74.7	84.0	86.0	83.3	83.3	80.0	81.3
GPT-4.1 [108]	98.7	97.3	84.0	91.7	84.7	94.0	89.3	84.7	89.3	86.0	97.3	90.7
GPT-4o [55]	99.3	88.7	84.7	90.6	83.3	90.7	87.3	91.3	84.7	94.0	100.0	90.4
Claude-3.7 Sonnet Thinking [2]	93.3	95.3	88.0	92.2	90.7	94.7	94.0	94.0	89.3	87.3	92.7	92.0
Claude-3.7 Sonnet [2]	94.0	94.0	86.7	89.4	88.0	95.3	86.7	94.0	94.0	88.0	90.7	91.0
Claude-3 Opus [56]	97.3	98.7	95.3	97.8	96.0	100.0	96.0	97.3	96.0	94.7	99.3	97.1
Gemini-2.5 pro-exp [60]	98.7	96.0	94.0	97.2	95.3	94.7	94.7	97.3	92.0	95.3	98.0	95.8
Gemini-2.0 flash-thinking-exp [59]	82.7	72.0	62.0	70.0	62.0	72.0	66.0	74.0	58.0	62.7	82.7	69.5
Gemini-1.5-pro [58]	96.7	90.7	87.3	90.6	88.0	87.3	74.7	84.7	91.3	88.7	92.7	88.5
Grok-2-vision [109]	94.7	90.0	80.7	83.9	87.3	84.7	81.3	84.0	82.0	82.7	90.7	85.6
GLM-4v-plus [110]	68.0	89.3	84.0	80.6	68.7	75.3	84.7	82.0	82.7	92.7	66.7	79.5
Moonshot-v1-128k-vision [111]	92.0	78.7	83.3	82.8	80.7	84.0	78.7	81.3	83.3	82.0	93.3	83.6
hunyuan-vision [112]	62.0	64.7	64.7	58.3	58.7	68.0	68.0	57.3	69.3	53.3	54.7	61.7
Open Source MLLMs												
InternVL3.0-8B [14]	62.0	18.0	23.3	36.1	32.7	42.0	17.3	28.7	30.0	26.0	46.7	33.0
InternVL3.0-14B [3]	84.0	67.3	66.7	83.3	67.3	85.3	74.0	68.7	74.7	71.3	88.7	75.7
InternVL3.0-38B [3]	90.7	74.0	84.0	80.6	80.7	84.0	89.3	80.0	85.3	73.3	90.0	82.9
InternVL3.0-78B [69]	89.3	79.3	86.7	83.9	80.0	90.7	82.7	78.7	87.3	74.0	93.3	84.2
Qwen2.5-VL-7B-Instruct [4]	46.7	18.7	23.3	30.0	26.7	24.7	12.7	20.0	15.3	22.0	45.3	26.0
Qwen2.5-VL-32B-Instruct [4]	95.3	91.3	88.0	87.2	84.7	94.7	85.3	85.3	89.3	90.7	92.0	89.4
Qwen2.5-VL-72B-Instruct [4]	88.7	75.3	82.7	81.7	83.3	86.7	74.0	79.3	71.3	76.7	91.3	81.0
DeepSeek-VL2-tiny [113]	66.7	62.7	61.3	58.9	52.7	63.3	51.3	46.7	60.7	70.0	68.0	60.2
DeepSeek-VL2-small [113]	0.0	85.3	88.0	85.0	92.0	86.0	81.3	88.0	90.0	94.7	85.3	79.7
DeepSeek-VL2 [113]	88.7	98.0	88.7	89.4	89.3	91.3	85.3	89.3	90.0	94.0	83.3	89.8
LLaVA-OneVision-7B [114]	84.7	90.7	84.7	83.9	87.3	83.3	90.7	86.0	94.0	88.0	86.0	87.1
LLaVA-OneVision-72B [114]	86.0	83.3	76.7	86.7	80.7	85.3	73.3	82.7	87.3	81.3	89.3	83.0
Average Valid Rate	82.9	78.6	78.0	80.9	77.4	82.1	77.1	78.6	79.7	79.1	84.9	80.0

Notably, the 27B model was loaded using `float32` precision due to stability issues encountered with half-precision inference at this scale. In contrast, the 2B and 9B models were loaded using `float16`, enabling faster evaluation with lower memory consumption. This discrepancy in numerical precision should be considered when interpreting performance differences, as it may influence numerical stability and output variance in borderline cases. Overall, the performance differences across the three model scales are relatively modest, with the 27B model achieving the highest average success rate but only slightly outperforming the 9B variant. Given its strong balance between accuracy and efficiency, we selected TxGemma-Predict-9B as the default evaluator in our benchmark. It provides competitive results comparable to the 27B version while offering significantly lower memory and runtime overhead than full-precision large-scale inference.

M Evaluation of Molecular Structure Validity

As shown in Table 13, current general-purpose MLLMs exhibit relatively high overall valid rates, typically exceeding 60%. Similar to the success rate trends presented in the main text, reasoning-enhanced models (e.g., GPT-o1/o3/o4-mini[1, 107]) perform comparably to standard MLLMs (e.g., GPT-4.1/4o[108, 55]). For open-source models such as the InternVL3.0 series, the valid rate also tends to increase with larger model scales.

N Supplementary Reflections and Future Research Directions

N.1 Benchmark and Task Scalability

Although ToxiEval currently covers a diverse range of toxicity endpoints, there remains substantial room for expansion. Future benchmarks may incorporate more complex mechanisms such as chronic toxicity, genotoxicity, and metabolism-induced toxicity and multi-scale evidence from *in* and *vivo* studies to improve clinical relevance and real-world complexity. Additionally, while the current evaluation pipeline relies entirely on automated criteria, future versions may benefit from a hybrid human-in-the-loop system that combines automated screening with expert validation, enhancing reliability and interpretability.

N.2 Toxicity Endpoint Stratification

Experimental results reveal a clear stratification in toxicity repair success rates across different tasks, following a pattern of “easily repairable – moderate – high-bottleneck” difficulty. Tasks such as hERG_C and ToxCast show high success rates, while Tox21 and ClinTox fall in the intermediate range, and tasks like LD50, DILI, and SkinRxn exhibit consistently low repair rates. This distribution suggests that different toxicity mechanisms impose heterogeneous demands on molecular generation and that current general-purpose MLLMs struggle to model particular toxicological knowledge adequately.

N.3 Potential Negative Impacts and Ethical Considerations

Although current MLLMs have not yet achieved practical-level performance on toxicity repair tasks, their ability to efficiently generate molecular candidates at scale—particularly under unsupervised or low-supervision conditions—demonstrates substantial promise. This capability holds clear positive value for accelerating early-stage drug discovery. However, it also raises critical concerns regarding potential misuse. For instance, similar techniques could be exploited for designing illegal drugs with structurally evaded toxicity signatures or masked harmful properties, thereby increasing regulatory difficulty and societal risk. To address these concerns, we recommend that thorough ethical assessments, security audits, and regulatory safeguards accompany future efforts toward model deployment and public accessibility. It is essential to anticipate potential misuse pathways and implement proactive oversight mechanisms to ensure that technical progress aligns with legally compliant and socially responsible innovation in drug development.

O Case Examples of Successful Toxicity Repair

This section presents representative cases of successful toxicity repair using the Claude-3.7 Sonnet [2] model. For each primary task in the ToxiMol benchmark, one repaired molecule is randomly selected and visualized using its 2D molecular structure. All selected examples have passed the full ToxiEval evaluation criteria.

P License and Usage Information for External Assets

Our framework relies on several external libraries and implementations for molecular property calculations and evaluations. We provide detailed license information for each asset below:

RDKit. [84] Our framework extensively uses RDKit (version 2023.9.6) for various molecular operations, including QED calculation, Lipinski’s Rule of Five evaluation (RO5), and molecular similarity computation. RDKit is an open-source cheminformatics software package released under the BSD 3-Clause "New" or "Revised" License. The official repository is available at <https://github.com/rdkit/rdkit>, and more information can be found at <https://www.rdkit.org>.

Synthetic Accessibility Score (SAS). [104] The implementation of the Synthetic Accessibility Score in our framework is based on the work by Ertl and Schuffenhauer, as described in their paper "Estimation of Synthetic Accessibility Score of Drug-like Molecules based on Molecular Complexity and Fragment Contributions" (Journal of Cheminformatics 1:8, 2009). The implementation is adapted from the original code provided by the authors, which has been made publicly available. The SAS

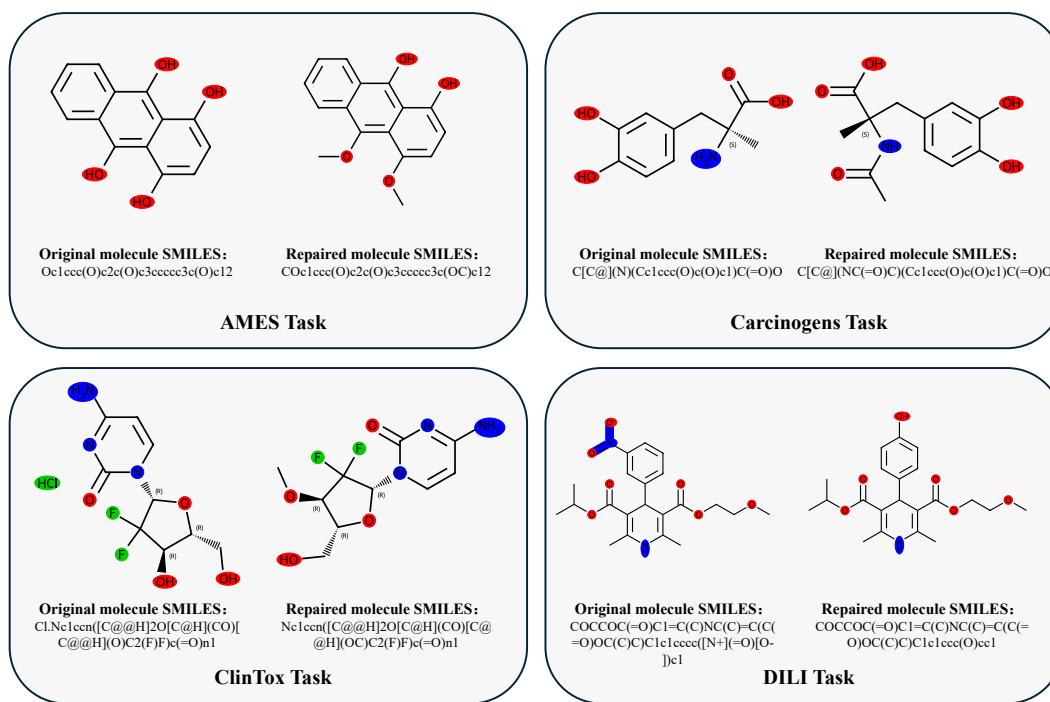


Figure 8: Representative examples of successful toxicity repair for AMES, Carcinogens, ClinTox, and DILI.

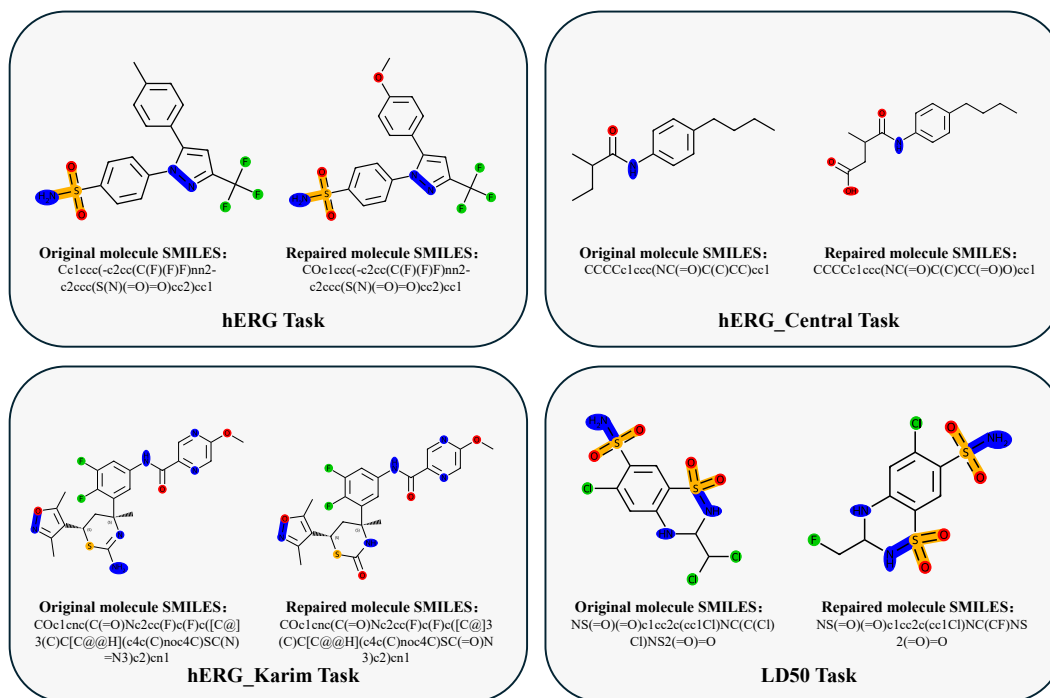


Figure 9: Representative examples of successful toxicity repair for hERG, hERG_Central, hERG_Karim, and LD50.

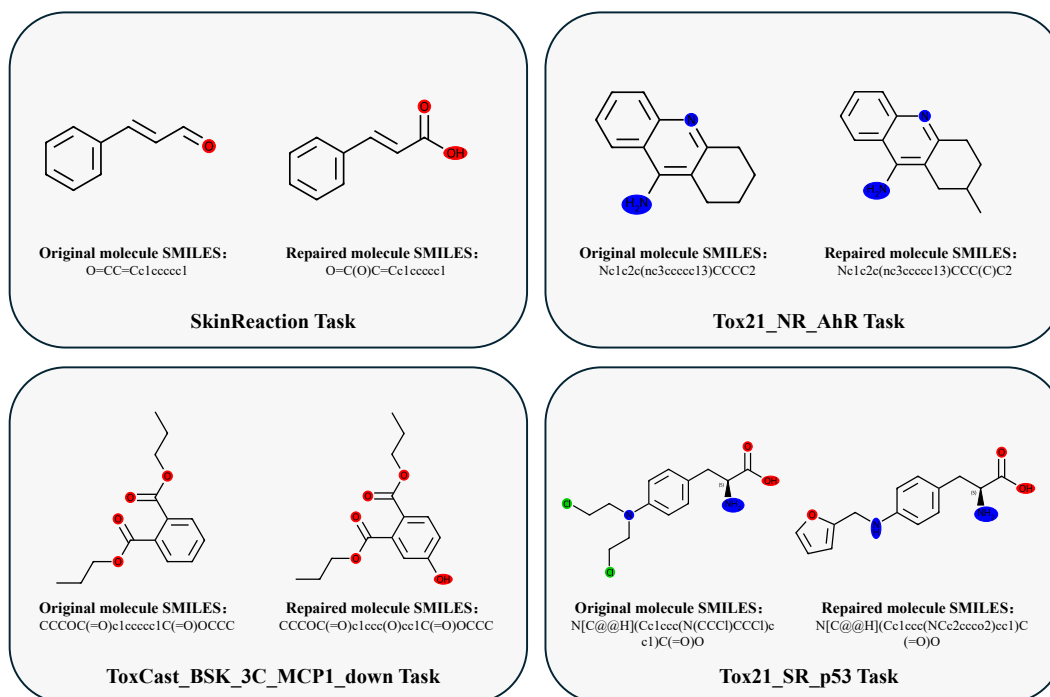


Figure 10: **Representative examples of successful toxicity repair for SkinReaction, Tox21_NR_AhR, Tox21_SR_p53, and ToxCast_BSK_3C_MCPI_down.**

implementation is released with the same BSD 3-Clause License as RDKit, as it's typically distributed as part of the RDKit control package. The original paper is available at <https://doi.org/10.1186/1758-2946-1-8>.

TxGemma. [38] Our framework uses the TxGemma-9B-predict model from Google for toxicity prediction, accessible via the Hugging Face Transformers library. Unlike standard open-source models, TxGemma is governed by the Health AI Developer Foundations Terms of Use rather than the Apache 2.0 license. The model can be accessed at <https://huggingface.co/google/txgemma-9b-predict>, with usage terms available at <https://developers.google.com/health-ai-developer-foundations/terms>. The official GitHub repository provides additional implementation details and usage examples: <https://github.com/google-gemini/gemma-cookbook/tree/main/TxGemma>. A full model description is available in "TxGemma: Efficient and Agentic LLMs for Therapeutics" by Wang *et al.* (2024), at <https://arxiv.org/abs/2504.06196>.

All external assets were used by their respective licenses and terms of use.